A review on functional applications of polyphosphazenes as multipurpose material for lithium-ion batteries

Journal of Energy Storage 85 (2024) 111049

Contents lists available at ScienceDirect

Journal of Energy Storage

journal homepage: www.elsevier.com/locate/est

Review article

A review on functional applications of polyphosphazenes as multipurpose material for lithium-ion batteries

Zhengping Zhao [a], Zhao Xu [b], Jiayi Chen [a], Mingqiang Zhong [b], Jiahao Wang [c], Jia Wei Chew [d,e,*]

[a] Zhijiang College, Zhejiang University of Technology, Hangzhou 310024, China
[b] College of Materials Science and Engineering, Zhejiang University of Technology, Hangzhou 310014, China
[c] College of Energy Engineering, Zhejiang University, Hangzhou 310027, China
[d] School of Chemical and Biomedical Engineering, Nanyang Technological University, 637459, Singapore
[e] Chemical Engineering, Chalmers University of Technology, 412 96 Gothenburg, Sweden

ARTICLE INFO

Keywords:
Polyphosphazenes
Lithium batteries
Polymer electrolyte
Electrode materials

ABSTRACT

Polyphosphazenes, which are inorganic-organic hybrid polymers with P═N as the skeleton, are well-known for their unique physicochemical properties stemming from their backbone structure and highly active P—Cl bonds. The diverse functional properties of polyphosphazene make it a promising research prospect in many fields, including solid polymer electrolytes, anode materials, diaphragms and so on. This review discusses the main synthesis routes, modifications for a variety of functions, as well as template precipitation self-assembly polymerization. Among them, template-induced precipitation self-assembly is an outstanding strategy for polyphosphazene to form nanospheres, nanosheets, and nanotubes. Solid state lithium batteries are promising energy storage candidates, but the Li^+ conductivity of the commonly used PEO electrolytes is limited to 10^{-6} S·cm^{-1} at room temperature. Polyphosphazenes-based electrolytes with an ether oxygen side tend to possess better ionic conductivity and are flame retardant. The polyphosphazenes organic polymer is also an attractive carbon material precursor and a good choice for anode electrodes. After high-temperature carbonization, N, P heteroatoms doped in-situ on the carbon matrix can change carbon neutrality and endow charged sites, further improving the lithium storage ability. In addition, polyphosphazene has potential for use on the diaphragm and other battery systems.

1. Introduction

Allcock et al. successfully synthesized soluble linear polyphosphazenes in 1965 and promoted the subsequent development of a variety of polyphosphazenes in the following decades [1]. In contrast to other hybrid polymers, polyphosphazenes have a modifiable inorganic polymer backbone structure to confer wide-ranging properties, because the constituent P and N atoms exhibit a unique conjunction of electrons to allow for varying side groups. The stability of the main chain and the easy adjustment of the side groups enable polyphosphazene materials to readily carry out various functional designs by changing the structure and grafting different functional groups. Therefore, polyphosphazene plays unique and advantageous roles in different applications and fields, as demonstrated by various studies. For example, polyphosphazene exhibits excellent performance as flame-retardant additives. Also, its superior biocompatibility has attracted more and more attention in the biomedical field, and its P and N doping characteristics have been used to improve the energy density of energy storage systems [2,3]. Unsurprisingly, polyphosphazene has been gaining attention as a promising material suitable for wide-ranging applications.

Lithium-ion batteries (LIBs) are recognized as one of the most efficient clean energy storage devices. Solid polymer electrolytes (SPEs) have been a promising research direction to eliminate thermal instability by replacing liquid electrolytes, as well as to enhance energy density and power density further [4]. Allcock et al. were the first group to confirm that the polyphosphazenes are very suitable as solid electrolytes, possessing advantages such as low glass transition temperature (Tg), a flexible and stable molecular structure to facilitate chemistry modification, etc. By nucleophilic substitution of ether sodium salt, the first-generation polyphosphazene electrolyte poly (bis (2-(2-methoxy ethoxy)-ethoxy) phosphonitrile (MEEP) was created, whose ionic conductivity was 2–3 orders of magnitude higher than that of poly

* Corresponding author at: Chemical Engineering, Chalmers University of Technology, 412 96 Gothenburg, Sweden.
E-mail address: jia.chew@chalmers.se (J.W. Chew).

https://doi.org/10.1016/j.est.2024.111049
Received 15 December 2023; Received in revised form 23 January 2024; Accepted 20 February 2024
Available online 24 February 2024

(ethylene) oxide (PEO) [5–7]. However, the ionic conductivity of the polyphosphazene solid electrolyte is still lower than that of traditional liquid electrolyte at room temperature, which makes it deficient for practical needs. Additionally, because the molecular chain of MEEP material is flexible, it is challenging to create a film with a stable size. This is a key problem needed to be solved urgently in polyphosphazene solid electrolyte at present.

The anode electrode is another important component of LIBs. Graphite, the common anode material, has remarkable cycling stability but a mere specific capacity of 372mAh/g, which restricts large-current and high-rate applications of LIBs. Dopants such as N, P and S have been proven to improve the lithium-embedded capacity of carbon materials [8,9]. Wu [8] used hexachlorocyclophosphazene (HCCP) as dopants in (graphene oxide) GO to improve the charge-discharge performance and showed that the capacity reached 1002mAh/g at the current density of 100 mAg^{-1}. However, when the N atom concentration exceeded a certain threshold, the continuous graphene structure was found to be damaged by N atoms, leading to significant drop in the conjugated electron cloud density, which affects the electrical conductivity of the anode material. In addition, polyphosphazene is also used as a binder for negative electrode particles to improve the structural changes during cycling. Si anode is considered a promising anode material for lithium-ion batteries because of its high theoretical capacity and low discharge potential. However, its disadvantage is also well-acknowledged, in that the Si anode undergoes a large volume change during the cycle. In order to restrain the volume expansion, Hong et al. used NH3-neutralized poly [bis (4-carboxyphenoxy) phosphine] (PCPP-NH_3) and poly(ethylene glycol) bisamine (PEG-NH_3) to prepare a polyphosphazene-based polymer material, and used it as a binder for the Si anode. The cross-linking structure of the binder, and the hydrogen bond between polyphosphazene and Si surface, better limit the volume change of Si anode during the cycle, and improve the performance of the Si anode [10].

Polyphosphazenes have flexible morphology and structure regulation in the micro-nanometer construction process. The polyphosphazene precursor, in particular HCCP, copolymerizing with for example 4,4-metonyl biphenol and 4,4-diamnophenyl-ether can introduce extra O and S heteroatoms. The nano-morphology of the polyphosphazenes is rather sensitive to solvents and temperatures, and can be transformed among nanospheres, nanotubes and so forth [11]. After being subjected to high temperatures, polyphosphazenes carbon materials with distinctive morphology, small size, and macroscopic quantum tunneling effects make excellent anode materials, aiding in the diffusion and arcing of lithium.

As an indispensable part of the lithium-ion battery, the separator plays a role in isolating the positive electrode from the negative one and only allows ions to pass through, thus preventing the battery from short-circuiting. To circumvent the problem of the traditional separator with respect to low affinity for electrolyte, nanoparticles have been shown to improve the poor electrolyte wettability of the separator because of their high hydrophilicity and large specific surface area. Xiao et al. [12] designed an in-situ limited polymerization technique with controllable size and distribution, in which HCCP and (4–4′-dihydroxydiphenylsulfone) BPS are used as comonomers, and highly crosslinked PZS microspheres (PZSMS) are uniformly loaded on vinylidene fluoride (PVDF) fibers. Compared with commercial (polyethylene) PE diaphragm, the resulting composite diaphragm was demonstrated to be a better lithium-ion battery separator with higher capacity retention and cycle stability, and excellent flame-retardant properties unique to PZS.

At present, there are few reports about polyphosphazene in the field of lithium-ion batteries. In view of the significant promise of this material in this field, a review is timely, which motivated the current work. Rothemund et al. reviewed the structure and synthesis of polyphosphazene in 2016 [11]. Zhou et al. reviewed the application of polyphosphazenes in the energy applications in 2023 [13]. In the current review, we comprehensively present the application of polyphosphazene materials in lithium-ion batteries, from micro- to macro-scale aspects, from design to synthesis, and from mechanism to application. Specifically, this is targeted at presenting and discussing the synthesis pathways, structure properties, morphology control and numerous electrochemical applications of polyphosphazenes (Fig. 1).

2. Structure and characteristics of polyphosphazenes

2.1. Electronic structure of polyphosphazenes

The general chemical structure of polyphosphazenes is shown in Fig. 2 [6]. In addition to the σ bond between N and P, there are also four remaining electrons in each P═N monomeric unit, one of which is on the P atom's 3d orbital and another on the N atom's 2p orbital hybrid to form a symmetric dp-pp conjugate double bond. So the main chain of polyphosphazenes is relatively stable, and distinguished from the general carbon-chain polymers with the conjugated "island" π bonding [11]. Because there is no interaction between π bonds, the rotation of the P—N bonds is not hindered, and the d orbitals of the P atom can be freely substituted during rotation, which explains why polyphosphazenes backbones have good flexibility and properties of electronic insulators. When connected with solvating side chains (typically ether chains), polyphosphazenes have a great deal of potential to develop into a promising solid polymer electrolyte because of these structural characteristics.

The following features also need to be taken into account: (1) The P—N bond lengths are shorter than those expected for a single P—N bond. (2) Unless the side group or end group influences predominate, the bond lengths around a ring or along a short chain are similar or identical. (3) Six-membered rings have approximately the same stability as eight and higher-membered rings, even though some are planar and others puckered. (4) No electronic spectral absorptions from the skeleton are detectable throughout the visible region or at a wavelength above 220 nm in the ultraviolet, and the spectra are similar irrespective of the ring size or chain length. (5) If electron-supplying side groups are present, the skeletal nitrogen atoms are markedly basic and can coordinate with protons or transition metals. (6) X-ray photoelectron spectroscopy results show that core binding energies are relatively insensitive to side groups and ring size. (7) Polarographic reduction and electron spin resonance has shown that in linear polyphosphazenes only a very low barrier exists to torsion of the phosphorous-nitrogen bonds.

All these indicate that the skeletal bonding structure in polyphosphazenes is quite different from the situation found in electron-rich organic compounds. In other words, these compounds are neither unsaturated in the sense of nonconjugated olefinic organic species, nor aromatic like benzene. In fact, they represent a highly unusual form of bonding that is unique in chemistry.

2.2. Synthesis routes and structure design of phosphazenes

The general synthesis routes of the phosphazene macromolecule are presented in Fig. 3, resulting structurally in linear polyphosphazenes, cyclic polyphosphazenes and cyclolinear polyphosphazenes [8,9], or categorized as poly (alkyl) phosphazenes and poly (aryl) phosphazenes according to the state of -P═N- [11]. The study of polyphosphazenes can be traced back to the 1960s when the successful preparation of soluble linear [$NPCl_2$] n (polydichlorophosphonitrile, PDCP) by Allcock and Kugel [1] was reported. PDCP is one of the most significant basic materials known as 'inorganic rubbers'. The synthesis routes of PDCP can be ring-opening polymerization [1], catalytic solution polymerization [14], a simply one-pot method [15], and controllable living cationic polymerization [16].

Ring-opening polymerization at high temperatures is one of the most common routes to synthesizing the PDCP. The mechanism is such that chlorine atoms are cleaved at high temperatures from HCCP, which is a six-membered ring alternately connected by P, N single and double bonds [1]. However, the molecular weight of the resulting product is

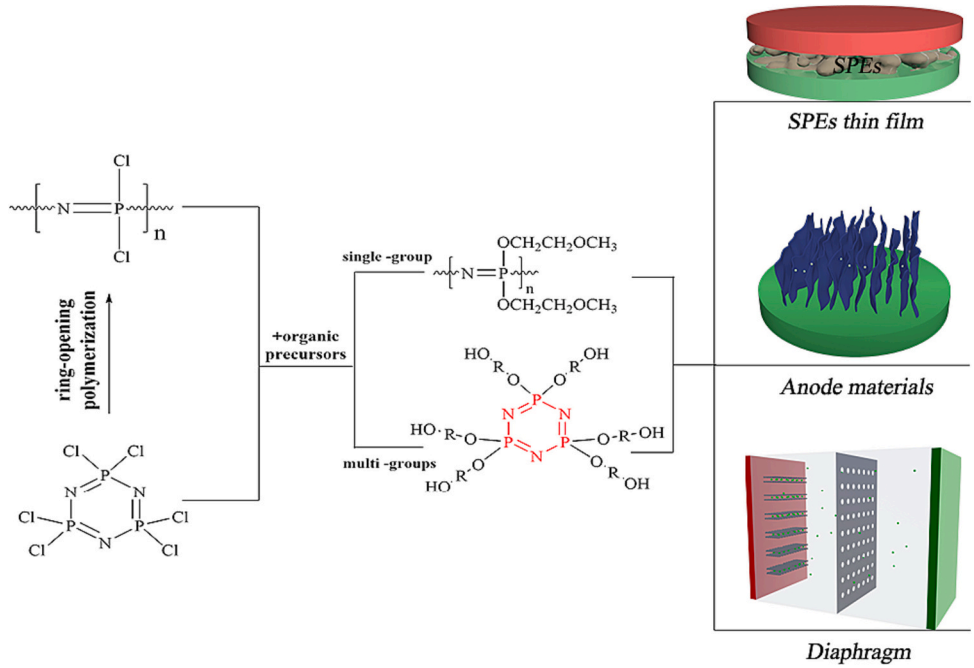

Fig. 1. General fabrication routes leading to various applications of polyphosphazenes.

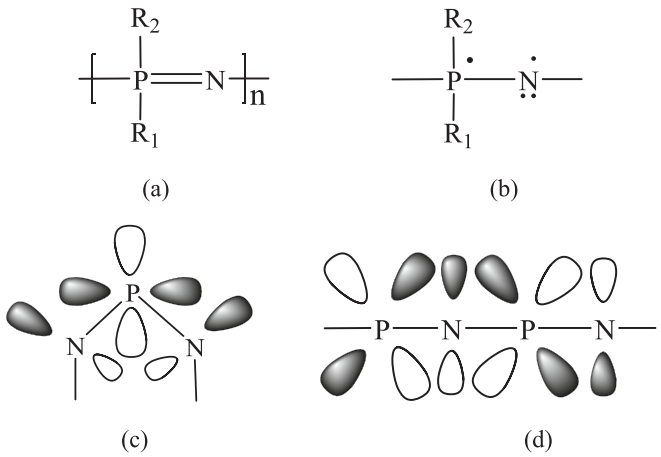

Fig. 2. (a) Chain structures and (b) electronic orbit of polyphosphazene derivatives. (c) In-plane and (d) out-of-plane pi-bonding between phosphorus 3d-orbitals and nitrogen 2pz-orbitals.

relatively high and with broad polydispersity, which is due to the uncontrolled Cl cleavage rate under the high reaction temperature that is essential to ring-opening polymerization. Accordingly, catalysts have been used to lower the reaction temperature without negatively affecting the reaction rate. Lewis-acids such as $AlCl_3$ and BCl_3 are a kind of efficient catalyst to moderate the Cl cleavage rate and reduce the required temperature.

A simple one-pot route has been developed in the presence of $HSO_3(NH_2)$ as a catalyst and $CaSO_4{\cdot}2H_2O$ as a promoter. Considering that $[N_3P_3Cl_6]$ is also prepared from the reaction of PCl_5 and NH_4Cl, linear PDCP can be directly synthesized from NH_4Cl and PCl_5 as monomers [15]. The one-pot method can not only prepare PDCP, but also prepare functionalized linear polyphosphazenes with OR groups replacing Cl. Rhili et al. used hexachlorocyclotriphosphazene and *p*-phenylenediamine as comonomers, and in the presence of triethylamine, highly crosslinked hybrid cyclotriphosphazene microspheres were prepared by the one-pot method to enhance the flame retardancy of epoxy resin [17]. Mehmood et al. synthesized cross-linked poly (cyclotriphosphazene-*co*-hesperetin) (PCTPP) microspheres by the reaction of hexachlorocyclotriphosphazene (HCCP) and hesperidin (HSP), and used them as drug carriers [18]. Also, under the action of accelerant and catalyst, the catalytic solution polymerization method, which is different from the one-pot method, involves ring-opening polymerization from $[N_3P_3Cl_6]$ in solvent 1,2,4-trichlorobenzene. The PDCP prepared by this method is not branched, and its yield is about 30 %.

Cationic active polymerization has a long history of being an effective synthesis method. It was found that Trichlorophosphoranimine ($Cl_3PNSiMe_3$) can be carried out as the monomer instead of HCCP, allowing good control of the polymerization of PDCP [19]. As shown in Fig. 4(a_2), in the presence of initiator PCl_5, $Cl_3P{=}NSiMe_3$ forms a cationic species $[Cl_3PNPCl_3]^+PCl^{6-}$ accompanying the loss of side product $[Cl_3SiMe_3]^+$. Furthermore, monomer $Cl_3PNSiMe_3$ can be polymerized by this cationic species to produce polymer chains with a 'living' cationic end group. The final polymer products with the expected molecular weight and extremely narrow molecular weight distribution are made possible by the living polymerization mechanism.

Under mild experimental conditions, there are numerous other ways to make PDCP, but long-chain PDCP alone is insufficient for practical application. By replacing the Cl atom with nucleophilic moieties that have one or more nucleophilic sites, functional groups can be added to the side chains of polyphosphazenes, taking advantage of the high chemical activity of Cl on the P atoms. This results in the formation of inorganic-organic hybrid polymers [11].

Some common substitution routes are shown in Fig. 4(b). These nucleophilic moieties include alkoxides, aryloxides, amines, fluoroalkoxy, etc. It is this flexible selection of side groups that gives easy access to freshly prepared precursor PDCP, which acts as a source for numerous differently functionalized proteins shown in Fig. 5. Researchers have been very interested in these highly versatile materials, whose properties can be varied from plastic to rubber, from insulator to electrolyte, and from water-solubility to water stability, leading to uses in a variety of fields including biomedicine [20], flame retardant materials [21], energy materials [22], and others [23,24].

There are several specific examples of functional phosphazenes modified by different substitutions and their applications in different fields. A representative antioxidant polyphosphazene is shown in Fig. 4

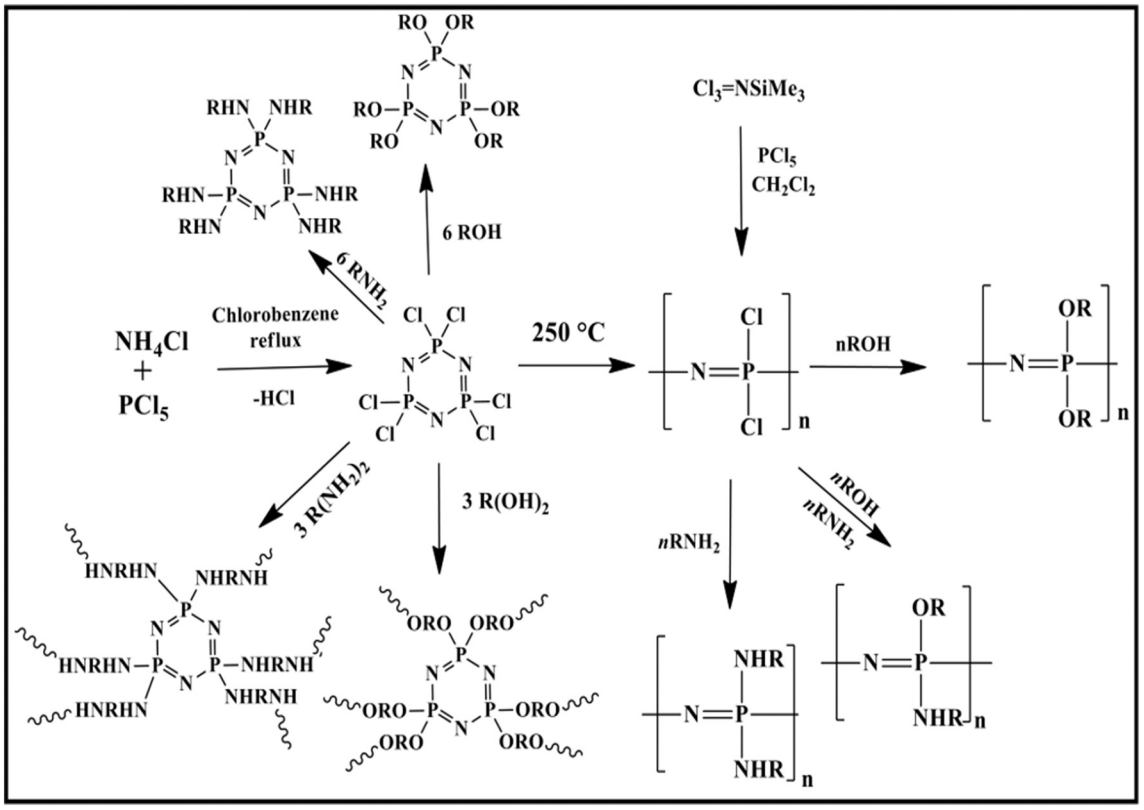

Fig. 3. General synthesis schemes of polyphosphazenes by SN_2 nucleophilic substitution mechanism.

(c_1). Specifically, leveraging the ferulic acid units to provide antioxidant character and ethyl esters of amino acids to increase the hydrophobicity, the antioxidant polyphosphazene prepared was an excellent scaffold material for tissue engineering [25,26]. Because linear polyphosphazene has good biocompatibility and can break down in the body into non-toxic phosphoric acid small molecules [20], it is ideally suited to serve as the basis for active pharmaceutical ingredients. Qiu grafted diisopropylamino and PEG segments onto the PDCP backbone to obtain pH-responsive amphiphilic polyphosphazenes (Fig. 4(c_2)), in which diisopropylamino reversed drug resistance [27]. Mayer-Gall grafted allyl alcohol onto PDCP via sodium allyl alcohol (Fig. 4(c_3)) to synthesize poly (allyl) phosphazenes, which were then blended onto cotton or polyester fibers [28]. The modified fabrics showed good flame retardancy and high limiting oxygen indices due to the high content of phosphorus and nitrogen in polyphosphazenes [29]. Allcock et al. substituted polyphosphazene with 2-(2- methoxyethoxy) ethoxy and lithium sulfonimide, and demonstrated superior high ionic conductivity, which was attributed to the contribution of 2-(2- methoxyethoxy) ethoxy to cation transport and the increase of lithium sulfonimide to charge carrier concentration. When used in energy storage, this not only meets the requirements for ionic conductivity, but is also safe [6].

Although many modifications can be made to obtain useful phosphazenes, almost all of them are random polymers because substitutions are likely to be non-selective and thus it is difficult to prepare ordered block polymers. And it is difficult to ensure the complete replacement of Cl atoms due to the steric hindrance and polar strength of the substituents, which is especially obvious in the mixed substitutions process. Also, undesired phenomena can occur for multi-functional groups polymers, whereby the already attached side chain R_1 is replaced by R_2. For ordered block copolymers of phosphazenes, the cationic active species $[Cl_3PNPCl_3]^+$ PCl^{6-} initiating active polymerization is considered one of the best preparation ways.

As shown in Fig. 4(d), by using unmodified or modified $R_3PNSiMe_3$ as a monomer and polymerizing it with the cationic $[Ph_3PNPCl_3]^+$ X^{6-}, it is convenient to prepare an ordered block copolymer. The key to this polymerization is grafting the desired groups onto the $Cl_3PNSiMe_3$ as functional monomers that are able to maintain $[Ph_3PNPCl_3]^+$ X^{6-} chemical activity. In addition, block copolymers combining a polyphosphazene segment with a second polymer segment can also be synthesized. Weikel et al. attached Br $(CF_3CH_2O)_2PNSiMe_3$ to the aminopolylactide terminus accompanying a small HBr molecule stripped off and then obtained a second polymer block (Fig. 4(e) - product 1) [30], which was used to respond to cationic active centers that already contained the phosphine nitrile fragment (Fig. 4(e)- product 2), thereby prepared polylactide–poly(dichloro-phosphazene) block copolymers (Fig. 4(e)- product 3). The prepared backbone includes polylactic acid organic block, which aids in hydrolysis, in addition to providing the phosphine nitrile inorganic block with a firm structure.

The controlled polymerization craft allows the synthesis of polyphosphazenes with more complex architectures. The active end-group like amine-capped -[N=PCl_2]- is a better option when considering the restriction of incomplete substitution of long-chain phosphazenes because it is grafted on the backbone of other alkanes to form densely grafted molecular brushes. Another benefit is the length and functionalization modification of branched phosphazenes can be designed and adjusted in advance. In addition, 1,1,1-tris (diphenylphosphino) methane could be used as an excellent multifunctional core for the parallel growth of star polyphosphazene, as shown in Fig. 4(f) [31]. Tris (diphenylphosphino) methane could be completely ionized by the chlorophenomeric agent C_2Cl_6, which would then produce $[RPh_2PCl]^+$ living cationic species with Cl counter ions. Just like the cationic active polymerization mentioned before, the three active chains initiate $Cl_3PNSi(CH_3)_3$ monomers to bind together to form the *star*-like polymer, and the [N=PCl_2] attached can be further nucleophilically replaced, finally synthesizing the dendrimers macromolecular. These block copolymers [32], star polymers [33], comb polymers [34], and spiral polymers [11] developed in recent years have been noted for their special molecular structures, which not only contain the inherent

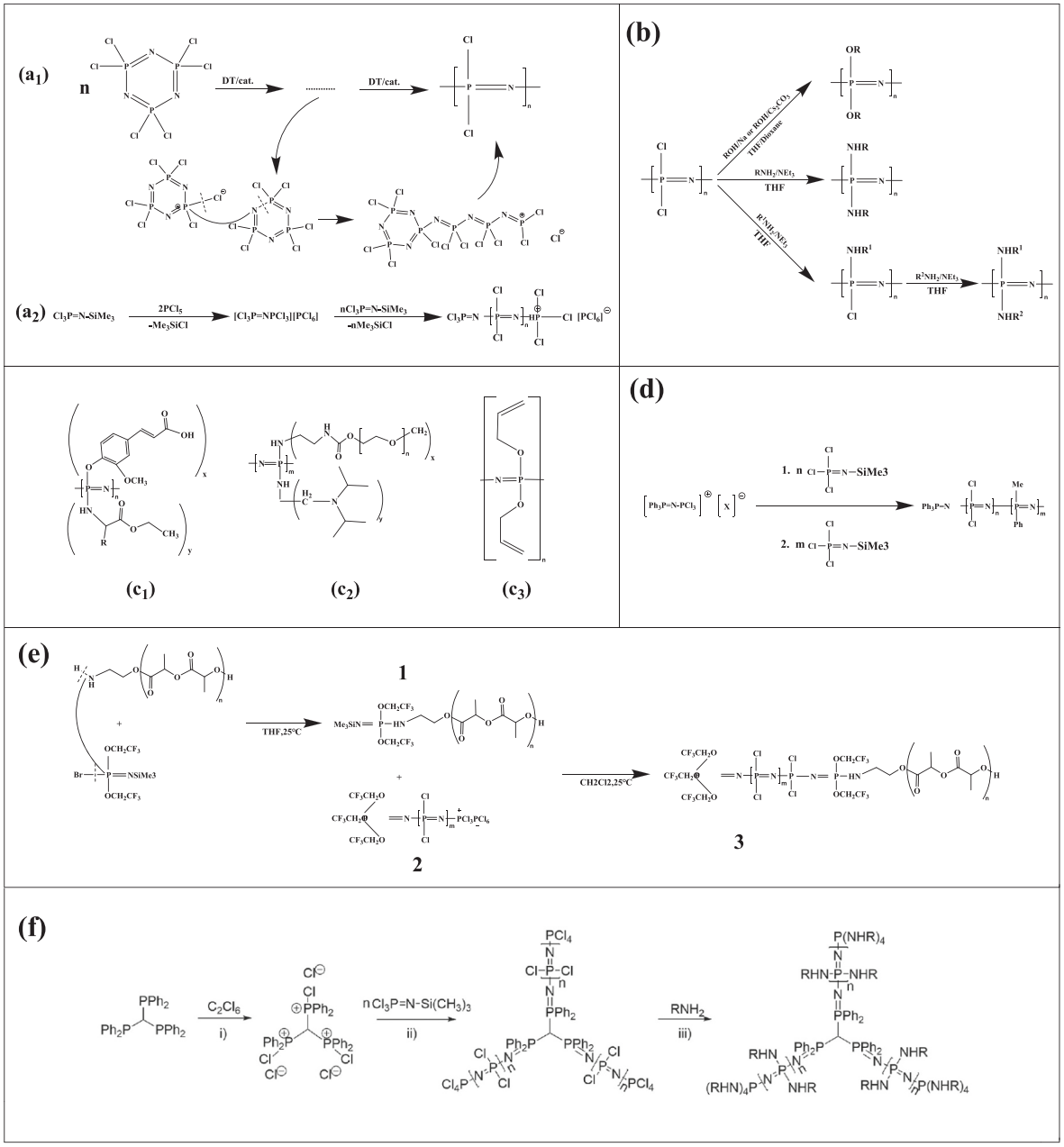

Fig. 4. (a_1) Thermal and/or catalytic induced ring-opening polymerization of PDCP. (a_2) The living cationic polymerization of PDCP [11]. (b) The most common method to substitute polyphosphazene from reactive precursor PDCP [11]. Several specific examples of functional phosphazenes modified by different substitutions: (c_1) the antioxidant polyphosphazenes and (c_2) PH-responsive amphiphilic polyphosphazenes and (c_3) poly (allyl) phosphazene for modifying fabric [25,27,29]. Copyright 2012, American Chemical Society. (d) Synthesis of poly (dichlorophosphazene) and poly (alkyl/aryl) phosphazene block copolymers [11]. Copyright 2016, American Chemical Society. (e) Synthesis route of polylactide–alanine substituted polyphosphazene block copolymer [30]. Copyright 2010, Royal Soc Chemistry. (f) Synthesis of three-arm stars-liked polyphosphazenes [31]. Copyright 2016, Wiley-Vch.

characteristics of organic-inorganic hybrids but also deliver interesting application potential with the amphiphilic function that can self-assemble to form micelles and aggregate.

Due to the abundance of P—Cl bonds, HCCP is also a very significant raw material in addition to PDCP, particularly for the cyclic polyphosphazenes whose reaction mechanism is based on precipitation polycondensation. For insoluble polyphosphazene nanoproducts made from HCCP and other multi-functional nucleophiles, such precipitation polycondensation is a notable in-situ polymer method [35].

During the process, an acid acceptor like triethylamine (TEA) is required to absorb the byproduct hydrogen chloride (HCl) lost from HCCP, thereby promoting the reaction. It is worth to note that a byproduct of the reaction called molecular triethylamine hydrochloride (TEACl) can act as a template to affect the final morphology of highly crosslinked polyphosphazenes [36]. Cyclomatic polyphosphazenes prepared through in-situ precipitation polycondensation express unexpected sensitivity to the morphology control via changing the induced template [9]. Tang prepared polyphosphazenes with different morphology including hollow nanotube [35], nanofiber [37], and nanospheres [38] by changing the solvent and temperature factors (Fig. 6(a)–(d)). The nanostructure endows polyphosphazenes with a high specific surface area and a large number of active sites. The surface effect and quantum size effect of nanomaterials have important research value in the fields of electrocatalysis, biomedicine [20,39] photothermal [40,41] flame retardant [42], and proton exchange membrane [9].

Polyphosphazenes are a sort of heteroatomic co-doped matrix. Lone

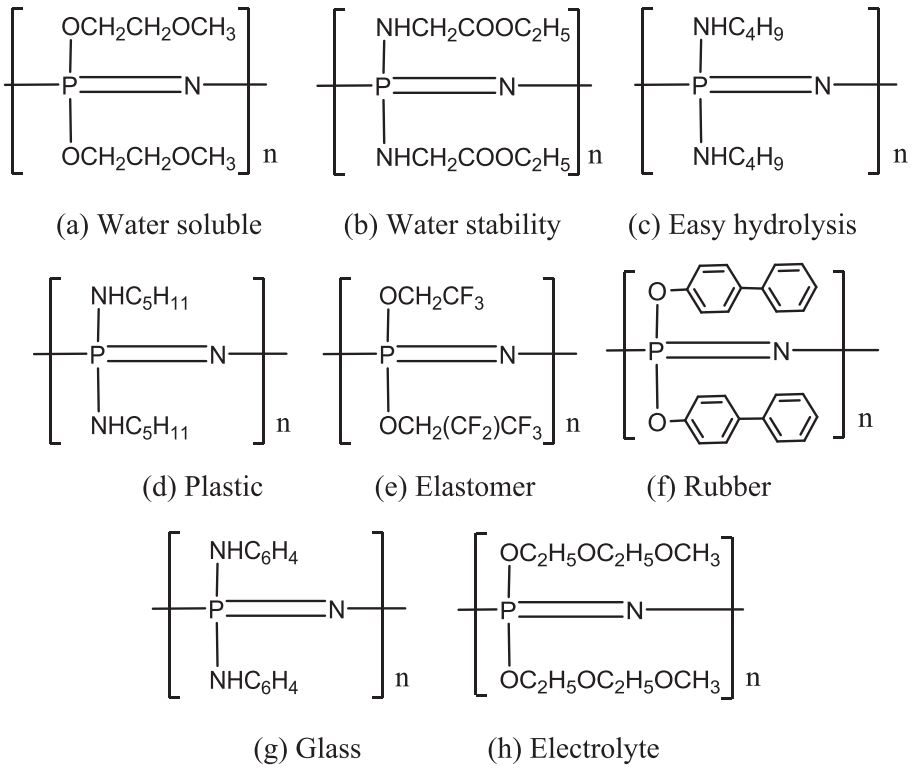

Fig. 5. Functionalization of polyphosphazene materials.

pairs of electrons in N are beneficial to coordinate metal ions. Wang et al. [43] reduced $AgNO_3$ in situ on the surface of polyphosphazenes nanotubes to obtain PZS@Ag nanoparticle composites, as shown in Fig. 6(g), and the TEM images clearly show anchored Ag nanoparticles evenly distributed on the surface of PZS nanotubes can contribute to improving the catalytic activity.

In summary, polyphosphazene is a kind of inorganic-organic hybrid polymer with P═N as the skeleton. The stable dP-pP conjugate formed between N and P atoms ensures the stability of the main chain, and the substitutable Cl atoms in its side groups makes it extremely adjustable. Various preparation methods, different functional designs and different forms of polyphosphazene materials have aroused remarkable academic interest, resulting in the development of many such materials with different characteristics and applications, spanning both hydrophobic and water-soluble materials, and applications ranging from flame retardant to biological to energy storage.

3. The application of polyphosphazenes in lithium batteries

In the past few decades, new energy applications have received significant attention. When compared to other battery systems, lithium-ion batteries (LIBs) stand out as highly efficient electricity-producing tools that can meet the demands of high energy density, excellent rate performance, long cycle life, and relatively low cost. However, several drawbacks, including liquid leak, inflammable and explosive hazard of traditional electrolytes, as well as inadequate capacity of electrode material, hamper further widespread use. In order to overcome these difficulties and enhance the overall performance, a significant amount of literature related to polyphosphazenes have emanated, mainly in solid polymer electrolytes, anode material and diaphragms.

3.1. Solid polymer electrolyte

Liquid electrolytes, such as ethylene carbonate (EC), diethyl carbonate (DEC), etc., are popular for beneficial characteristics including (i) excellent solubility of high concentration lithium salt (up to 1.0 M); (ii) good conductivity at room temperature (higher than 10^{-3} S·cm^{-1}; (iii) low viscosity and low melting point [44,45]. Unfortunately, there are also downsides to liquids, such as leakage, flammability and requiring bulky enclosures. In contrast, solid polymer electrolytes (SPEs) have superior safety performance, are lightweight, are more portable, have film-processing properties and have excellent interface contact [46].

SPEs are mixtures generally consisting of polymer matrix and soluble inorganic lithium salts LiX (where X = I, Cl, Br, ClO_4, CF_3SO_3, BF_4, AsF_6, etc.) [48], serving both as the separator to prevent the electrodes from shorting contact and as the significant ion conductor. It is worth mentioning that SPEs have a lower value of relative permittivity than polar liquid electrolytes when used in lithium batteries. The ion transport mechanism of SPEs is closely relative to polar groups such as —O—, =O, —S—, —N—, —P—, C═O, C≡N mainly on the polymer side chain [26]. Take the polyphosphazenes as an example, the coordination and discoordination processes between the migrating lithium cation and oxygen atoms occur constantly through the movement of molecular chain segments, thereby assisting the intra-chain and inter-chain diffusion of lithium ions as demonstrated in Fig. 7(b).

The tricky part is that this ion migration mechanism requires a considerable amount of cation transference number derived from lithium salt whereas the anions remain loosely associated in the vicinity, giving rise to lower Li^+ mobility and transference number [47,49]. Therefore, single charged highly symmetric anions with low basicity as well as larger volume are preferred (Fig. 7(a)), which can delocalize even better and reduce the interference of anion. Moreover, some studies supposed that the N atoms on the backbone of polyphosphazene also have the analogous coordination effect like Li^+/O or are even stronger via forming a "pocket" structure as depicted in Fig. 7(c) [4,50]. There have been attempts to utilize density functional theory (DFT) and classical molecular dynamics (MD) simulations to investigate this ion transportation mechanism in terms of the bis (2-(2′-methoxyl)) phosphazene (MP) dissolving $LiBF_4$ as the research object [50]. The radial

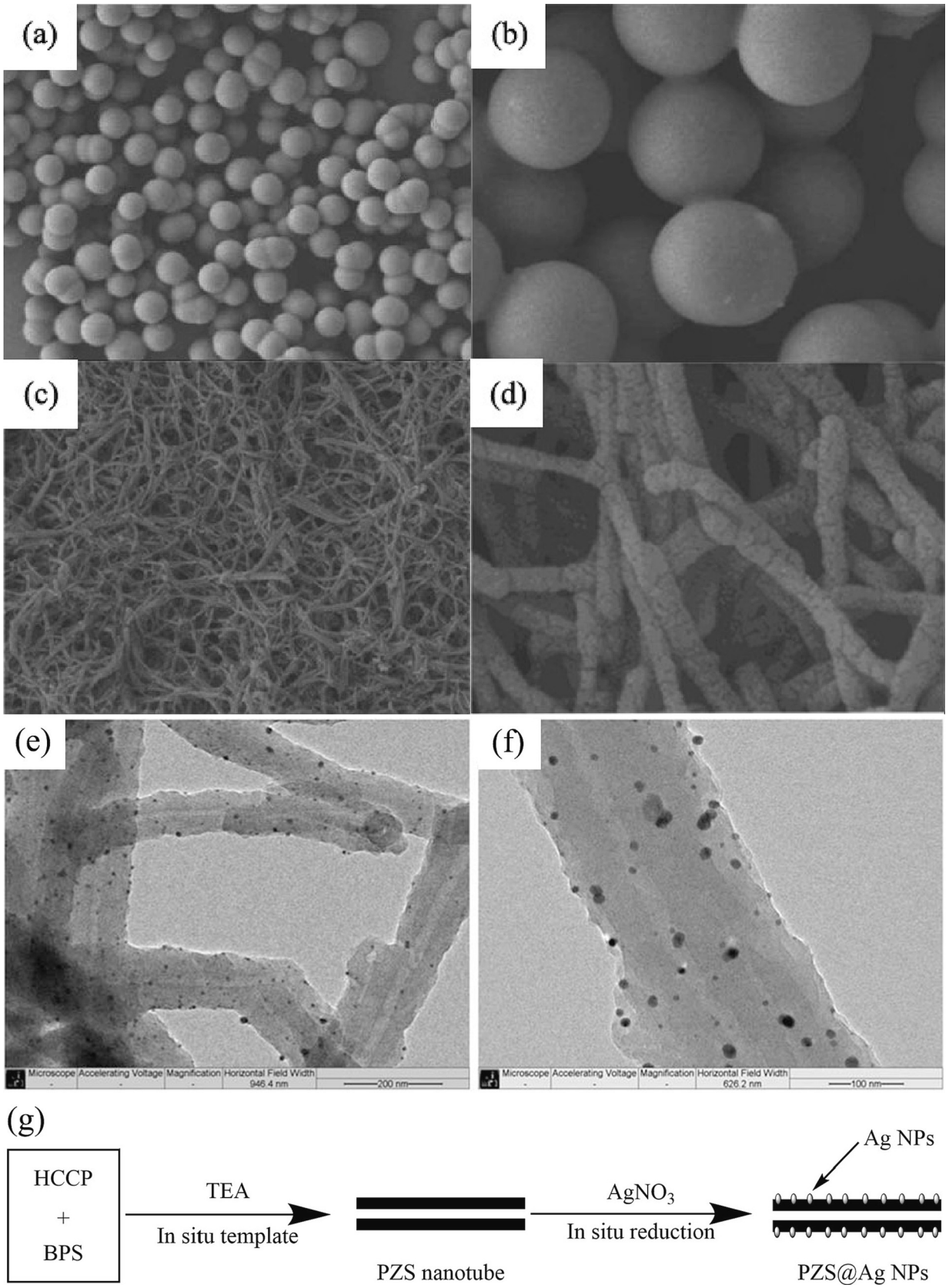

Fig. 6. SEM images of (a,b) nanospheres and (c, d) nanotubes of polyphosphazenes. TEM images of (e, f) PZS@Ag nanoparticle composites. (g) synthesis route of the PZS@Ag NPs [43].

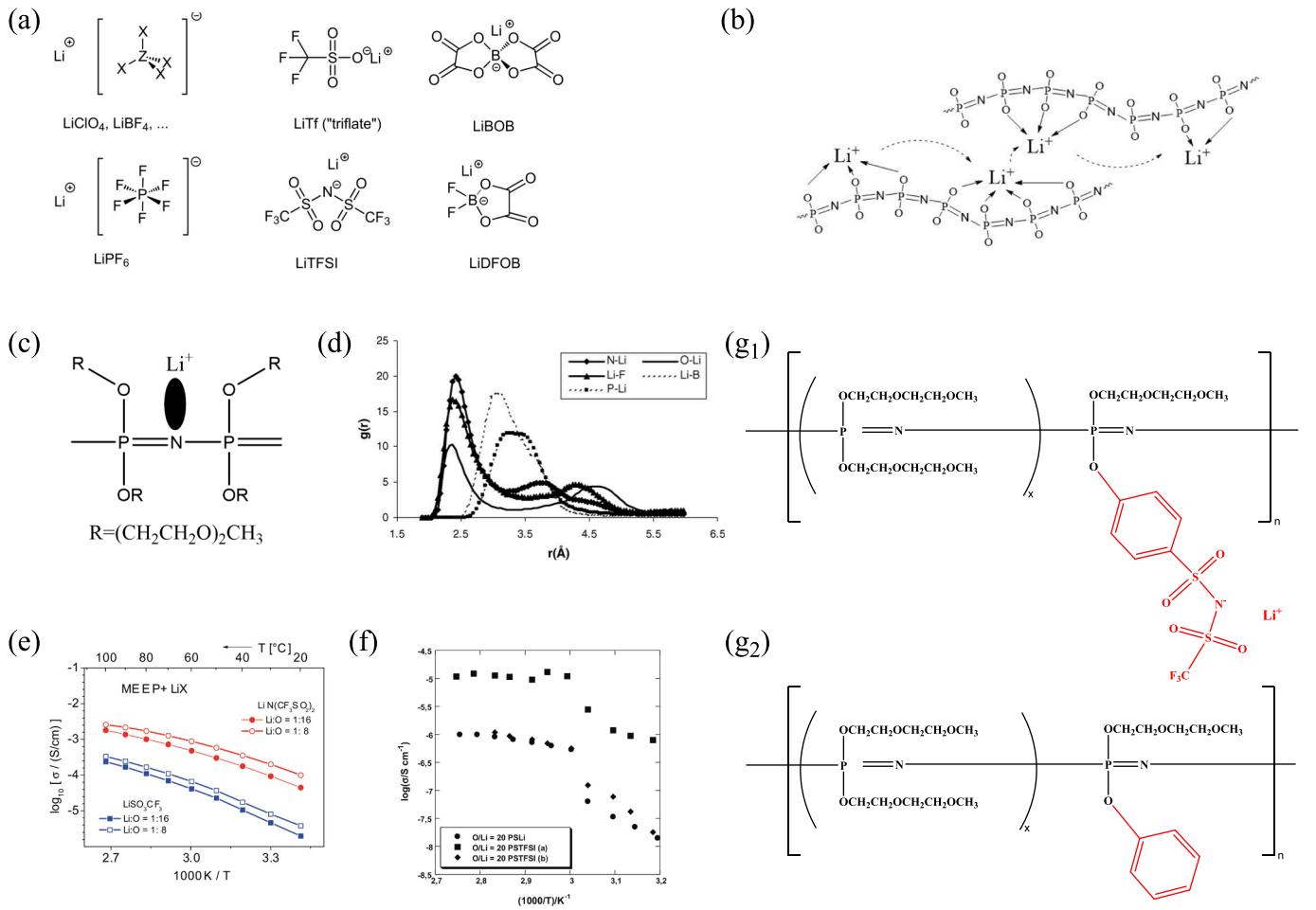

Fig. 7. (a) Lithium salts commonly used in polymer electrolytes [47]. Copyright 2013, ROYAL SOC CHEMISTRY. (b) Schematic of the segmental motion-assisted diffusion of Li^+ [50]. (c) Coordination of Li^+ with N and O atoms in 'pocket' structure [50]. (d) The Radial distribution functions from MD simulations of the MP-LiBF4 system at 400 K [50]. Copyright 2005, Elsevier. (e) The ionic conductivities of MEEP with LiTFSI and LiTf, respectively [47]. Copyright 2013, Royal Soc Chemistry. (f) Arrhenius diagram of ionic conductivity of polymer electrolyte PSTFSI varying with temperature [48]. Copyright 2011, Elsevier. The molecular structures of polyphosphazenes (g1) with 2-(2-methoxyethoxy) ethoxy and lithium sulfonimide substituent and (g2) with 2-(2-methoxyethoxy) ethoxy and phenoxy side substituent [7]. Copyright 2011, Elsevier.

distribution function gAB (r) is defined as the ratio of the real number of atoms B to the ideal number within a sphere of radius r around atom A. In other words, the higher the value of gAB (r) is, the more B atoms that may exist near atom A, and thus the stronger the interaction between them. As shown in Fig. 7(d), the first peak of gNLi (r) is much higher than that of gOLi within $r < 2.5$ Å and the ratio of the two peaks is about 2, indicating the closest neighbor N atoms more strongly interact with Li + than with ether O atoms. Moreover, the stronger interaction of Li^+/N was also found to not only promote the dissociation of ion pairs ($Li^+BF_4^-$) but also enhance the probability of inter-chain hopping of Li^+ ions [51].

For the wide variety of polymer electrolytes involved, it is difficult to use a universal physical formula to describe their structure and conductivity [54]. Currently, commonly used models include Arrhenius and Vogel-Tammann-Fulcher (VTF) [52].

The Arrhenius equation is usually used to explain the effect of the chain movement of amorphous polymers on ion-migration:

$$\sigma = \sigma 0 e^{\frac{-Ka}{kT}} \quad (1)$$

whereby the pre-exponential factor σ_0 is related to the carrier, and the linear least square fitting of the σ-T^{-1} figure can be used to calculate the ion conductance activation energy Ea. The smaller the Ea value is, the more active the ions, and thus the better the conductivity.

Different from the Arrhenius formula, the VTF equation describes the ionic movement behavior above Tg more specifically

$$\sigma = \sigma_0 T^{-\frac{1}{2}} e^{-\frac{B}{T-To}} \quad (2)$$

where B represents the activation energy of electrical conductivity and T_o is the reference temperature of Tg - 50 K [4].

Since the first report of poly (ethylene oxide) (PEO) alkali metal salt complexes as polymer electrolytes by Fenton et al. in 1973 [53], PEO's low Tg and high flexibility at room temperature have made polymer electrolytes a popular choice among solid electrolytes [54]. Li^+ can form a strong dipole interaction with the etheroxy group on the chain and move through the ethylene oxide (EO) chain in the amorphous region to conduct ion diffusion [55]. But the conductivity of PEO is only 10^{-6}–10^{-8} S·cm^{-1} at ambient temperature [46], and its oxidation limited potential is only 3.8 V, which cannot match with high voltage window cathode materials like $LiCoO_2$.

Because bonding angles of the inorganic backbones −P=N− are less restricted without long-range conjugate effect as compared to carbon-based chains, polyphosphazenes have thermal stability and good compatibility with no electrochemical reaction. The molecular main chain of polyphosphazenes has excellent high elasticity and a low glass transition temperature (−90 ~ −50 °C), giving segmental mobility at room temperature or lower temperatures [43]. The above advantages make polyphosphazenes promising as polymer electrolyte matrices. But

the polyphosphazenes must still meet the following necessary conditions as the supporting framework of electrolyte and ion transfer medium: (i) the conductivity of Li^+ at room temperature is close to 10^{-4} S·cm^{-1}; (ii) high lithium ion mobility, with the Li^+ migration number as close to 1 as possible; (iii) high chemical and thermal stability; (iv) stable mechanical strength; and (v) compatibility with electrode materials, environmental benign and non-toxic [4,44].

Allcock et al. first made a preliminary study on polyphosphazenes as solid polymer electrolytes [5]. They used 2-methoxy ethanol, 2-methoxy ethoxy ethanol and other kinds of alcoholic sodium salt to replace active chlorine atoms, thereby synthesizing polyphosphazenes with an ether oxygen (EO) group on the side chain. In the same $LiBF_4$ electrolyte system, the simulated diffusion rate of etheroxy polyphosphazenes could reach 1.5×10^{-5} cm^2·s^{-1}, slightly higher than PEO (Table 1) [50]. As mentioned earlier about the lithium-ion migration mechanism in the polyphosphazenes backbone, the high segmental mobility of the backbone and its flexibility helps polyphosphazenes possess better ionic conductivity than PEO. But dissolving the lithium salts still depends on the ether oxygen side chain. Poly (bis (2-(2-methoxy ethoxy) -ethoxy) phosphonitrile (MEEP) with ether oxygen side chain is one of the most fundamental polymer electrolytes via completely nucleophilic substitution by diethylene glycol monomethyl ether sodium salt. The flexible –[$PR_2 = N$]– group kept MEEP in amorphous state over a wide range of low temperatures, resulting in MEEP being a transparent highly viscous liquid. Compared with carbonic polymers, the torsion barrier of the MEEP backbone chain is much lower. The ionic conductivity of MEEP is 10^{-5} S·cm^{-1}, 2–3 orders of magnitude higher than PEO (Table 1). In addition, the inherent thermal stability and flame retardancy of MEEP is also required for the LIBs system [40,56].

In addition, compounding polyphosphazene with PEO is also a promising method to explore new polymer electrolytes. Zhang et al. introduced organic–organic hybrid poly (Cyclophosphazene-*Co*-4,4-sulfoyldiphenol) (PZS) microspheres with active hydroxyl groups into polyethylene oxide (PEO), resulting in a new polymer electrolyte (CPE). The experimental results show that the polyphosphazene microspheres can effectively improve the ionic conductivity of PEO-based electrolyte [57].

3.2. Enhancing physical and chemical properties

For several decades, numerous researchers have worked towards improving the physical and chemical properties of polyphosphazenes electrolytes, including the choice and use of lithium salt, copolymerization/crosslinking, single ion conductive polymer electrolyte, the addition of plasticizer and filler, etc. In the following, these types of research will be explored and the different factors influencing the ionic conductivity will be analyzed.

(i.) *Selection of lithium salt*

Based on the cationic active polymerization of linear polyphosphazenes supported by Manner [58], Paulsdorf prepared MEEP/$LiCF_3SO_3$ homogeneous polymer electrolyte with different lithium salt content [59]. Merely by 5 % lithium salt addition, the ionic conductivity was enhanced by 50 % at room temperature to 10^{-5} Scm^{-1} without significant Tg change. The type of lithium salts selected influences the phosphonate markedly. Comparing LiTFSI and LiTf (Fig. 7(a)) in the same MEEP system, Fig. 7(e) shows that LiTf gave almost an order of magnitude of lower conductivities as compared to LiTFSI, as the high dissociation degree of LiTFSI is more helpful to the freedom and migration of lithium ions.

Table 1
Comparison of simulated diffusion rate and ionic conductivity between MEEP and PEO.

	Simulated diffusion rate (cm^{2}S^{-1})	Ionic conductivity (Scm^{-1})
MEEP	10^{-5}	10^{-5}
PEO	10^{-7}	10^{-6}–10^{-8}

(ii.) *Single-ion polymer electrolytes*

Apart from the lithium salt types, the combination methods of lithium salt on the polymer electrolyte as well as the additive amount are important factors. Most of the polymer electrolytes reported so far are double ionic conductors, and both cations and anions can move freely. The coordination between lithium cations and polar atoms, mainly EO in the polymer chain, leads to faster and easier migration of anions, resulting in a lower actual migration number of lithium ions (<0.5). The migration of anions not only causes corrosion and degradation of the electrode surface but also causes self-discharge. In order to reduce the migration of anions, the single-ion polymer electrolyte system was developed by tethering the anionic covalent onto the rigid polymer chain. A single-ion polymer electrolyte PSTFSI has been synthesized with polystyrene backbone and $-SO_2N-SO_2CF_3-$ grafted group [48]. Interestingly, its ionic conductivity is almost 10^{-5} Scm^{-1} above 60 °C but only 7.94×10^{-7} Scm^{-1} at ambient temperature, as shown in Fig. 7 (f), which is far below that needed for practical use in LIBs. This is mainly attributed to the insufficient dissociation of Li^+.

In addition, Allcock has tried covalently linking the arylsulfonimide substituent to the backbone of polyphosphazenes to form single-ion polymer electrolytes and explored the effect of arylsulfonimide content on polymer electrolyte properties. The molecular structures are shown in Fig. 7(g_1, g_2), with the immobilized arylsulfonimide lithium salt acting as the source of lithium cations. It was found that ionic conductivities at 25 °C declined as the immobilized arylsulfonimide lithium increased (Table 2). Besides, the polyphosphazene with a phenoxy substituent was also synthesized and combined with the same dissolved salt LiTFSI but unbound forming non-single-ion polymer electrolytes, which could be used to compare with the former single-ion polymer electrolytes system. It was affirmed that non-single-ion polymer electrolytes have better ion conductivity of about an order of magnitude higher at 25 °C due to increased macromolecular motion associated with the less bulky phenoxy substituents. Comparatively, the increase of arylsulfonimide lithium substitution content in the single ion polymer system, and the increase of LiTFSI in the non-single-ion polymer system, were such that the ionic conductivities both express a mainly declining trend. The former was attributed to the restricted macromolecular movement and possible shielding of nitrogen atoms, but the latter was more due to the instant cross-linking state of Li^+ with EO confining lithium cation transferring [7]. The coordination structure formed by polar groups EO and Li^+ is subjected to competition between the solvation and the lattice energy of inorganic salts. Low lattice energy is conducive to the stability of the coordination structure. This is also evident from Table 2 and 3, showing that lower Tg and smaller Ea are related to a higher ion conductivity. Clearly, the correct lithium salt type, combination nature and the appropriate amount of lithium salt are important for obtaining better performance (Table 3).

Besides the lithium salt factor, the ether oxygen side chain also has a significant effect on lithium cation migration. Theoretically, ether oxygen side chains provide the polarity sites of EO that are directly related

Table 2
The relationship between aryl sulfonyimide content and Tg, Ea, and ionic conductivity [7].

Lithium sulfonimide (%)	Tg (°C)	Ea (kJ/mol)	σ at 25 °C (10^{-5} S·cm^{-1})	σ at 80 °C (10^{-5} S·cm^{-1})
5	−64	5.3	0.25 ± 1.2 %	2.8
9	−45	7.5	0.11 ± 0.6 %	3.5
19	−31	9.2	0.075 ± 0.4 %	5.0
22	−16	13.6	0.011 ± 0.1 %	2.2

Table 3
The relationship between phenoxy content and Tg, Ea, and ionic conductivity [7].

LiTFSI Mol (%)	Tg (°C) with no LiTFSI	Tg (°C) with LiTFSI	Ea (kJ/mol)	σ at 25 °C (10^{-5} S·cm^{-1})
5	−77	−72	4.3	4.0 ± 1.3 %
10	−73	−65	3.7	5.0 ± 1.6 %
15	−69	−54	5.5	4.0 ± 1.3 %
20	−66	−45	6.6	2.7 ± 0.7 %

to the solubility of lithium salt. A larger number of EO results in a stronger solvating capability and more migrated lithium cations. But a higher EO concentration ratio does not always mean improved conductivity or a higher cation migration number. Cations attached evenly with EO groups at a Li^+: EO concentration ratio of 1:8 but aggregated tightly at 1:4. It is the aggregation of ion pairs that limits the free movement of cations, which lowers the maximum ionic conductivity of the polymer electrolyte. Comparing the long-branch chain substituted JAPP [60] with the short-branch chain substituted PBMP [61] at the same lithium salt condition, it was found that the ionic conductivity of JAPP-based SPEs was rather close to that of the BMP-based ones at room temperature instead of the prediction that JAPP-based would be superior to BMP-based SPEs as shown in Fig. 8(a_1, a_2). This was ascribed to the flexibility of short branched chains enhancing polymer segment mobility and improving the intrachain/interchain transition of Li^+ [62]. It is a reasonable guess that the appropriate length of the side group not only is supposed to contribute to the dissociation of lithium salt but also can increase the mechanical stability of the salt-in-polymer solutions without the need of chain entanglement or cross-linking. As a result, the pursuit of a long side chain to get more polarity sites in EO is not inadvisable but actually reduces ionic conductivity instead [47].

(iii.) *Copolymerization/cross-linking*

Mechanical stability is also an important factor in ensuring the salt-in-polyphosphazenes system works. As mentioned above, polyphosphazene itself has excellent segment flexibility, but also requires a certain degree of structural stability and mechanical strength as the final salt-in-polymer electrolyte. How to find the balance between these two factors to achieve the best overall performance is the key question. Segmental activity refers to the movement and arrangement of different structural units in the molecular chain, while mechanical stability focuses on the deformation and failure resistance of materials under external stress. In order to balance these two aspects, the molecular structure and chemical composition of polyphosphazene materials can be modified. For example, the segmental activity of polyphosphazene materials can be controlled by controlling the length of main chain, side chain structure and crosslinking degree of polyphosphazene molecules, which changes the mechanical properties of the materials. At the same time, the mechanical stability of polyphosphazene can be enhanced by introducing suitable additives to improve its resistance to external stress. Since the polymer structure has a significant effect on Tg and chain motion, the simple linear structure cannot meet the high mechanical strength requirements of electrolytes. Polyphosphazenes with long branched chains or aromatic ring groups could provide the required mechanical strength through chain entanglement or stiff groups, respectively. Zhang comprehensively discussed and proposed that the improvement of mechanical properties comes at the cost of ion migration [63]. Fig. 8(b) illustrates the strengthening order of the mechanical strength and electrical and thermal stability of the architecture of the different polymers (i.e., linear < comb-like < hyper-branched < cross-linked polymers), but the ionic conductivity shows the opposite trend. Among these, cross-linking is a good method to get the optimal balance between mechanical stability and segment flexibility.

For a viscoelastic polymer such as MEEP with low Tg (−80 °C), it must be cross-linked by chemical method, ultraviolet ray or radiation irradiation to provide sufficient mechanical strength. Allcock has synthesized via an attractive route to combine the firm sol-gel derived silicate network with MEEP, integrating the firmness of silicon and the flexibility of MEEP for SPE_S [64].

Tsao et al. took Poly [(2-(2-methoxyethoxy) ethoxy)-2-(phenoxy) ethoxy phosphonitrile] MEEPP as a template polymer and changed its crosslinking degree to regulate the movement ability of the polymer chain segment [65]. It was found that MEEPP with 6 % crosslinking degree had the best ionic conductivity, reaching 5.36×10^{-5} S·cm^{-1} at 100 °C, as shown in Fig. 8(c, d). With the increase in cross-linking degree, better mechanical stability can be obtained, but the ionic conductivity of MEEPP significantly decreased because the movement of the chain segments is restricted. Besides, it was observed that MEEPP with 18 % crosslinking extent had no oxidation reaction even though the voltage was close to 7.0 V, whereas MEEPP with 6 % crosslinking extent had already undergone an intensive electrochemical reaction at about 6 V. This suggests that the electrochemical stability of cross-linked MEEPP strengthened with the increase of the degree of cross-linking.

(iv.) *Gel polymer electrolytes (GPEs)*

GPEs are formed by the polymer matrix with an electrolyte solution containing proper high-boiling solvents and/or plasticizers. It has been reported that the plasticizer can increase the amorphous region of SPEs, promoting the movement of chain segments and the dissociation of ion pairs, thus improving ionic conductivity [66]. However, the corrosion of the metal electrode and the reduction of film strength are problematic [44]. The most relevant problem is related to the high flammability and high vapor pressure of organic carbonates solvents, which may lead to hazardous explosions once they overheat. Common organic additives such as propylene carbonate (PC) are flammable due to their C, O and H element compositions, so non-flammable, non-volatile and highly conductive solvents play an irreplaceable role in GPEs [54].

With alkoxy phosphate as flame retardant plasticizer (P_4, general formulation: $O{=}P(OC_2H_4OCH_3)_2OCH_3$), the conductivity of the prepared MEEP-based GPE was as high as 9.9×10^{-4} S·cm^{-1} at 30 °C [56]. Table 4 lists studied compositions of such gels. The linear trendline of log (conductivity) versus 1000/T exhibits purely Arrhenius-type behavior, with higher conductivity accompanied by a larger proportion of P_4, clearly indicating viscosity, glass transition temperature and electrical conductivity have a strong relationship with plasticizers.

(v.) *Organic/inorganic composite polymer electrolytes*

It was discovered as early as 1983 that adding some fillers to a polymer electrolyte can increase ionic conductivity by two orders of magnitude [4]. The filler can be divided into two types, namely, active filler and passive filler. The active filler (G-$LiAlO_2$) can generate complex conductivity behavior. Whereas passive fillers such as Al_2O_3, SiO_2, and TiO_2 do not directly participate in the ion transport process, they play a role in reducing the crystallinity of the polymer matrix [48,62].

Kaskhedikar prepared poly [(bis (2-methoxyethyl) amino)1 − x (N-propylamino) x-phosphonitrile) (BMEAP) composite electrolyte membrane with homogeneous dispersion of nanometer Al_2O_3 (40 nm) [67]. It was found that the composite of Al_2O_3 nanoparticles enhanced the ionic conductivity by two orders of magnitude. The ionic conductivity at room temperature of 10^{-5} S·cm^{-1} is comparable to that of MEEP. Despite the volume of research work, the fundamental understanding has remained elusive. A hypothesis has been put forward that, by virtue of Lewis acid-base interactions with the filler surface, Li^+ could hop more freely both on the surface of the nanoparticles and/or polymer phase interface.

In summary, we need to consider the following key points when designing the salt-in-polyphosphazenes electrolytes system. Firstly, it is necessary for the ether oxygen side chain to be of appropriate length,

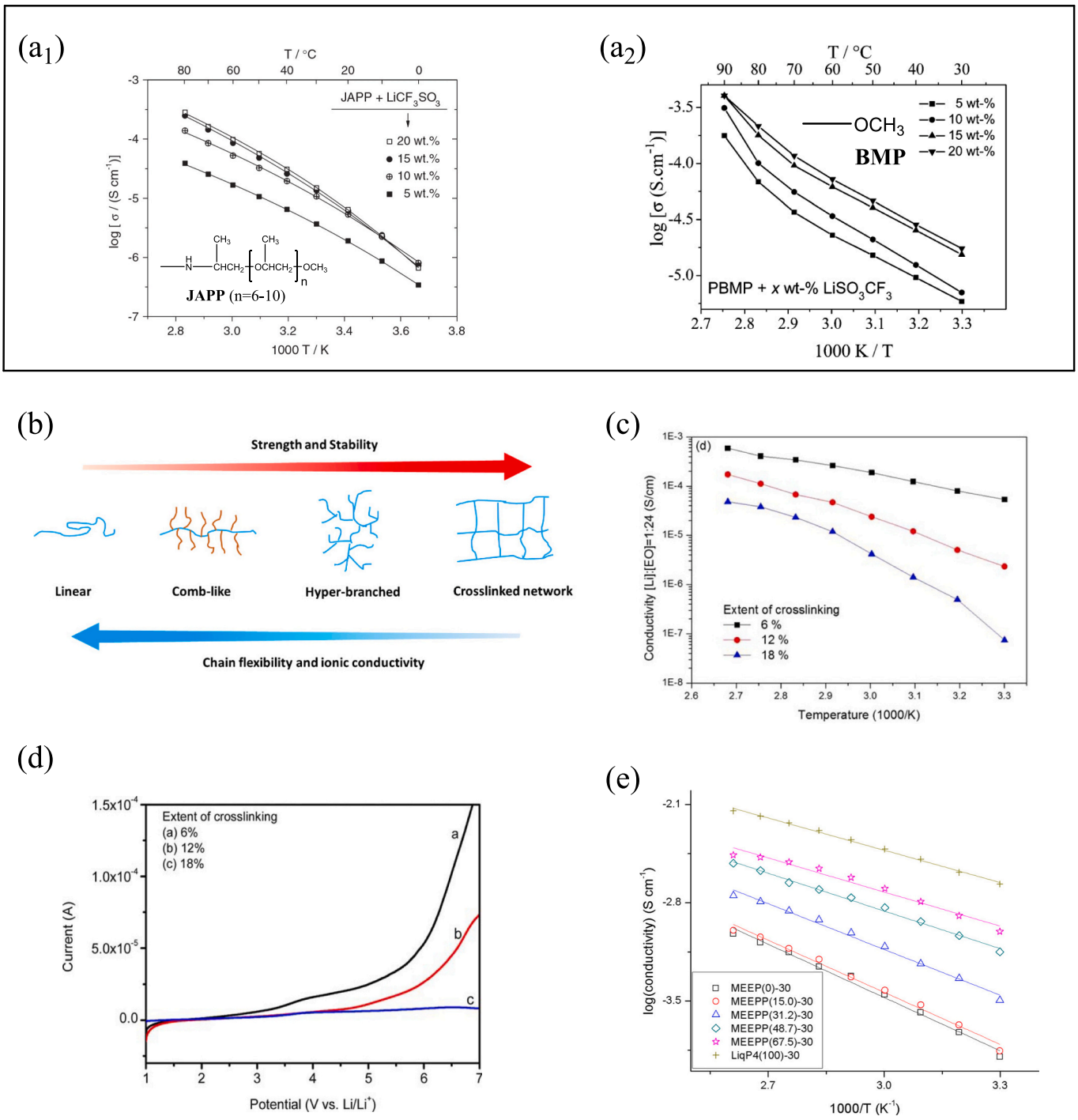

Fig. 8. Arrhenius plots for the conductivity of (a1) JAPP and (a2) PBMP with a variable amount of $LiSO_3CF_3$ [60,61]. Copyright 2006, Elsevier. Copyright 2008, American Chemical Society. (b) Effect of polymer structure type on electrolyte performance [63]. Copyright 2020, Multidisciplinary Digital Publishing Institute. (c) Ionic conductivity and (d) linear sweep voltammetry of MEEPP with different cross-linking extent at EO: Li^+ = 24:1 [57]. Copyright 2016, Wiley. (e) Arrhenius diagram of different gel-electrolyte samples [56]. Copyright 2013, American Chemical Society.

which is a prerequisite condition for the dissociation of lithium salt, but too many ether oxygen atoms would instead make lithium cation inactive. Secondly, the choice and usage of lithium salt have to be considered, noting that more polar lithium salts are more conducive to the mobility of lithium cations. Thirdly, crosslinking, solvents and/or plasticizers, organic/inorganic nanoparticles are all attractive modification choices that can improve the overall electrolyte performance of polyphosphazenes. So far, no solid polymer electrolyte has been explored to efficiently transport lithium ions at commercially viable levels (conductivities - 10^{-3} S·cm^{-1} at 25 °C). Electrolyte optimization requires further attention to physicochemical, thermal (e.g., Tg, Tm, degree of crystallinity), chemical (e.g., stability, compatibility), and electrical (e.g., ion transport number, ionic conductivity) parameters.

3.3. Anode materials

The most commonly used anode material at present is the graphite electrode [68]. Unfortunately, the specific capacity of graphite is

Table 4
Compositions of gel-electrolyte samples [56].

	MEEP (mol)	LiTf (mol)	P4 (mol)	P4 (mass %)	O/Li
MEEP (0)-30	1	0.2	0	0	30
MEEP (15.0)-30	1	0.25	0.25	15.0	30
MEEP (31.2)-30	1	0.33	0.66	31.2	30
MEEP (48.7)-30	1	0.5	1.5	48.7	30
MEEP (67.5)-30	1	1	4	67.5	30
LiqP4 (100)-30		1	5	100	30

relatively low (372mAh/g), and the diffusion rate of lithium between graphite layers is limited at between 10^{-9} and 10^{-7} $cm^2 \cdot s^{-1}$, which restricts application in the field of high energy density [69]. The goal was that the energy density of new energy batteries reach 400 Wh/kg by 2025 and 500 Wh/kg by 2030 [7]. To replace graphite and improve anode performance, many researchers have been looking for other materials with high capacity, excellent rate performance and necessary security [70]. According to the performance and reaction mechanism, three anode categories are listed as follows:

1) Intercalation/deintercalation materials: porous carbon, carbon nanotubes [71] and graphene [72], TiO_2 [73], $Li_4Ti_5O_{12}$ [74], etc.;
2) Alloy/non-alloy materials: Si [75,76], SiO [77], Ge, Sn, Al, Bi, SnO_2 [78], etc.;
3) Transition metal oxides (Mn_xO_y, NiO, Fe_xO_y [79], CuO, Cu_2O, MoO_2, etc.), metal sulfides, metal phosphides and metal nitride (M_xXy, X = S, P, N).

The most commonly used anode material in the market currently is graphite electrode. According to reports, P, S, B, N and other heteroatoms can effectively alter graphite's electrical neutrality and form six-membered heterocyclic compounds, which is beneficial to the electrochemical conductivity and lithium embedded capacity. For example, the N atom, compared with the C, possesses higher electronegativity, has a smaller atomic radius, and forms stronger interaction with Li, which are beneficial for Li^+ insertion. The induction property caused by doping is related to the content of the heteroatom. Ni has a high electronegativity, and the charge transport capacity was the highest when the doping amount of nitrogen was about 10 %. On the other hand, P has electron-donating characteristics, and the doping amount between 2.5 % and 6.7 % can provide ordered structure and improve the specific surface area. N, P and S ternary doping can produce a unique synergistic effect, offering superior electrochemical performance [50].

Zhong et al. prepared the yolk-shell structure MoS_2@PPN_S-C using PPN_S as the carbon skeleton, leading to a high specific capacity (883 $mAh \cdot g^{-1}$) of cycling stability at the current density of 100 $mAh \cdot g^{-1}$. DFT analysis shows (Fig. 9(d)) that N, P and S from polyphosphazenes can change the local charge density to generate more active sites, and the defects caused by doping can improve the electron transfer rate [80]. Besides, polyphosphazene-C was characterized as a typical mesoporous material via N_2 adsorption/desorption isotherm tests, with specific surface area up to 971.3 $m^2 \cdot g^{-1}$. It was prone to decomposition, giving rise to gas diffusing out from the inside of the flocculent structure formed by oligomers and small molecules during the pyrolysis process of polyphosphazene at low temperatures of 500–800 °C within the N_2 or Ar atmosphere. The large specific surface area and multi-channel structure dramatically contribute to ion diffusion, adsorption-desorption and effective contact of the reactive sites. So, the multi-porous carbon structure will be formed spontaneously without additional pore reamers and the original nanostructure can still exist stably with limited collapse phenomena [27].

Zhou [8] used HCCP as the precursor of PPN nanoparticles, as illustrated in Fig. 9(a, b, c). At a high temperature of 700 °C, HCCP covalently bonded with the hydroxyl group of GO, leading to ring-opening polymerization by itself to obtain uniformly dispersed PPN nanoparticles on the GO surface. The doping of P and N endows GO with excellent charge-discharge and magnification performance. The capacity of GO was up to 1002 $mAh \cdot g^{-1}$ at the current density of 100 $mAh \cdot g^{-1}$, and still maintained at 321 $mAh \cdot g^{-1}$ at the higher 5 $A \cdot g^{-1}$.

3.4. Diaphragm

As an indispensable component in a battery, the diaphragm acts as an isolation device between the positive and negative electrodes. It only allows ions to penetrate the diaphragm while forbidding the passage of free electrons, thus preventing short circuits in the battery [81]. At present, most commercial lithium-ion batteries use polyolefin microporous membranes (e.g., polyethylene (PE), polypropylene (PP)). Polyolefin diaphragms could provide stable mechanical/chemical properties and deliver high-temperature closed cell function, ensuring the thermal safety of lithium batteries [82]. The production technology of polyolefin diaphragms can be divided into dry process and wet process. The dry process is rather simple and economical with low pollution. But the regulation of pore size, distribution, and porosity is hard to standardize. What is worse is that the diaphragm is easily perforated [83]. On the other hand, the diaphragm synthesized through the wet process has a lower thickness, better air permeability and more even porosity, which can meet the requirements of miniaturization and the light weight of electronic products [84].

Excellent LIBs diaphragm generally needs to be equipped with the following requirements: (i) electrical insulation, which effectively prevents electrons from passing through; (ii) high mechanical strength and dimensional stability; (iii) chemical inactivity during the battery operation; (iv) favorable electrolyte wetting; and (v) suitable aperture size and uniform distribution of holes.

The polyolefin separator has a low affinity for the electrolyte, but good liquid storage capacity is required to provide the fast ion channel. It has been reported that, because of the high hydrophilicity and large specific surface area of nanoparticles, the poor electrolyte wettability of the diaphragm can be improved by filling [85] or coating [86,87]. Inorganic nanoparticles such as Al_2O_3, SiO_2 and TiO_2 also can effectively improve the mechanical strength, thermal stability and ionic conductivity of the diaphragm [63]. However, the problems of agglomeration and shedding of nanoparticles consistently persist.

Polyphosphazene with template-induced polymerization properties has been proven to be a good solution to the dispersion problem of nanoparticles. Fu et al. took HCCP and 4,4'-Sulfonyldiphenol (BPS) as monomers and triethylamine (TEA) as binding acids to synthesize cyclotriphosphazene-co-4,4-Sulfonyldiphenol (PZS) [88]. During the progress of the reaction, PZS was spontaneously and uniformly distributed on the surface of SiO_2, forming SiO_2-PZS nanoparticles with a core-shell structure, as shown in Fig. 10(g). Stirring prepared SiO_2-PZS with PVA and oxidized -β cyclodextrin, which was coated on both sides of the PE diaphragm. The core-shell structure of SiO_2-PZS significantly improved the dispersion of SiO_2 in the diaphragm. The ionic conductivity of PE-SiO_2@PZS diaphragm increased to 1.04×10^{-3} $S \cdot cm^{-1}$ compared with PE-SiO_2 (8.32×10^{-4} $S \cdot cm^{-1}$) and PE (8.25×10^{-4} $S \cdot cm^{-1}$). Hydroxyl groups on the surface of SiO_2-PZS not only enhanced the dissociation of lithium $LiClO_4$ but also contributed to the wettability of the diaphragm to accelerate Li + ion migration. The core-shell structure of SiO_2-PZS significantly improved the dispersion of SiO_2 in the diaphragm.

Lithium-sulfur batteries have a high energy density (2600 $Wh \cdot kg^{-1}$) and a good theoretical capacity (1672 $mAh \cdot g^{-1}$) [89]. However, the shuttle effect of soluble intermediates lithium polysulfide (LiPSs), including S_8, Li_2S_8, Li_2S_6, Li_2S_4, Li_2S_2 and Li_2S, results in active damping substances [90,91]. Various strategies have been proposed to mitigate the shuttle effect and improve battery performance, such as designing advanced cathode materials [92], anode protection [93], and the development of functional interlayers or diaphragms [94,95].

To this end, the unique planar non-conjugated six-membered ring

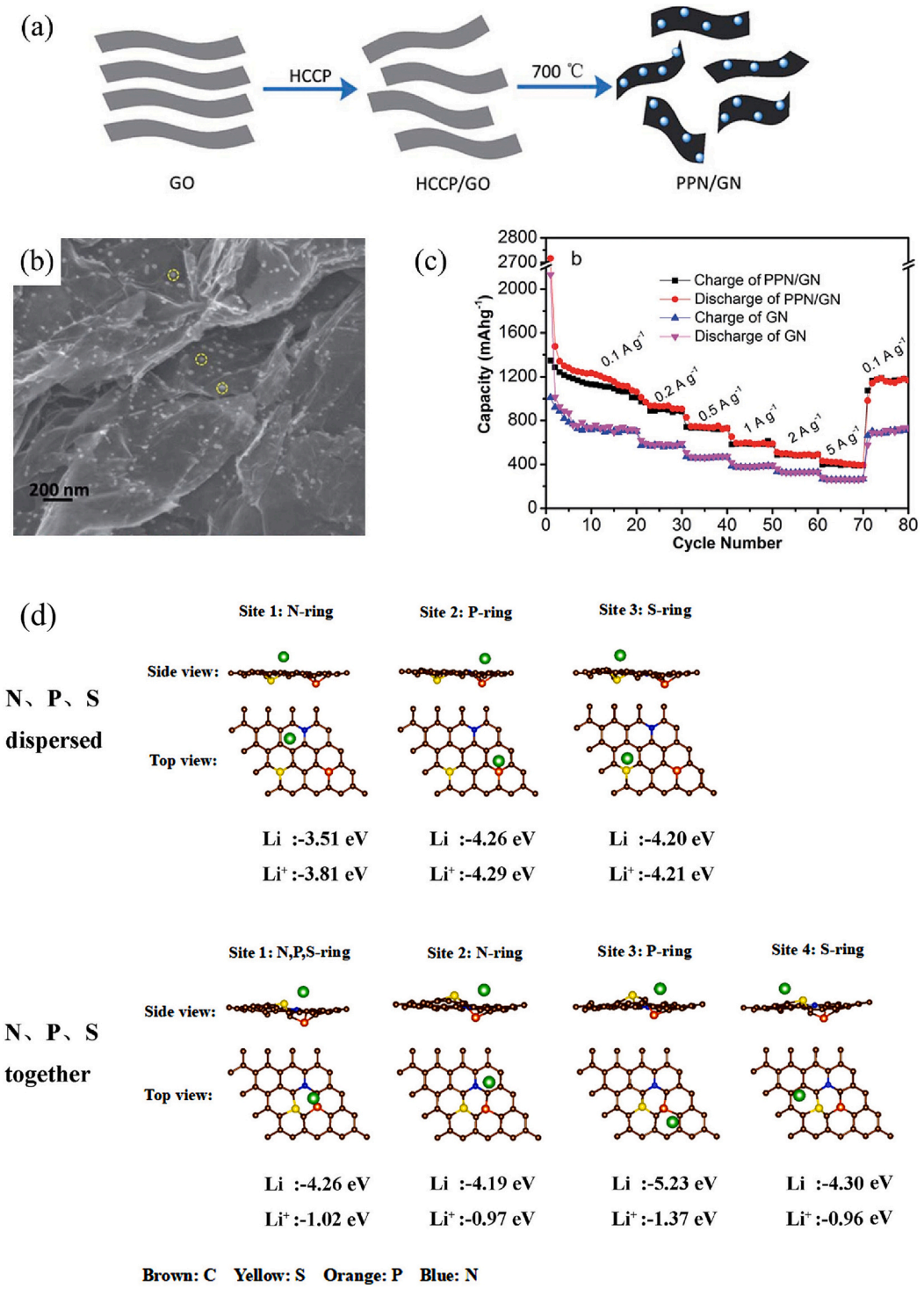

Fig. 9. The (a) synthesis strategy and (b) SEM image of PPN/GN [8]. (c) The rate capabilities of PPN/GN and GN electrodes at different current densities [8]. Copyright 2016, Royal Soc Chemistry. (d) The side and top views and binding energies of the N, P, S adsorption sites [80]. Copyright 2011, American Chemical Society.

structure of HCCP endows it with good flame retardancy and electrochemical stability [96]. Zheng grafted HCCP onto reduced graphene oxide (rGO) through chemical reaction between hydroxyl and active chlorine atoms, and then made it into a paste to be coated on the diaphragm [97]. The absorption band at 1018.8 cm^{-1} in Fig. 10(c) corresponds to the P-O(Ph) band, and 1163.1 cm^{-1} belongs to the characteristic absorption peak of C—P [98], proving that HCCP successfully grafted onto the rGO slice layer. Fig. 10(d) depicts the bonding state between HCCP and rGO. As shown in Fig. 10(f), the electrochemical performance of modified HCCP/rGO was significantly improved, and the reversible capacity was maintained at 565.2mAh/g after 130 cycles at a current density of 1 $A{\cdot}g^{-1}$. During the whole cycle, the coulomb efficiency was maintained at about 100 %, indicating that the composite has excellent electrochemical reversibility.

Zheng utilized density functional theory (DFT) calculations to analyze the interaction between HCCP and lithium polysulfide (LiPSs).

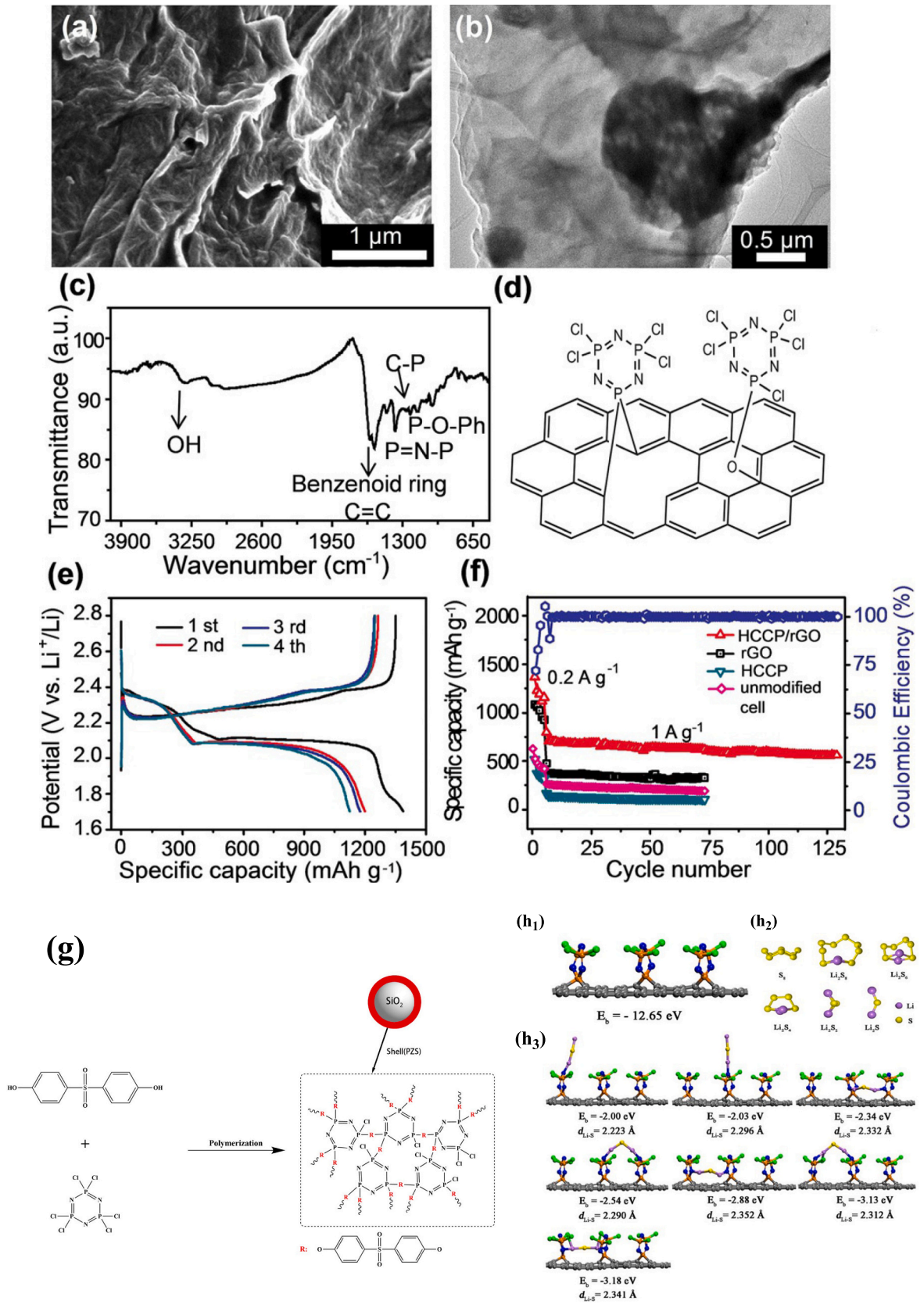

Fig. 10. (a) SEM and (b) TEM images of the HCCP/rGO composite [97]. (c) FT-IR spectrum and (d) molecular structure of the HCCP/rGO [97]. (e) Charge-discharge profiles and (f) the cycling performance of the cells with HCCP/rGO-coated, rGO-coated, HCCP-coated and unmodified separator [97]. (g) Synthesis scheme of SiO2-PZS nanoparticles [88]. Copyright 2018, Elsevier. (h1) The theoretical model structure of HCCPs/rGO. (h2) The li-S cluster model structure of each lithium stage. (h3) The structure model of Li2S absorbed on HCCP/rGO [97]. Copyright 2018, Wiley-VCH.

The binding energy statistics of LiPSs and HCCP/rGO absorbed at different sites were obtained, indicating that HCCP/rGO fixed LiPSs mainly through the Li—N bond [97]. The electron domain of rGO enhanced the electronegativity of the N atom, which increased its strong tendency to attract polar LiPSs. In particular, the structure remained intact when Li_2S was absorbed at different sites.

3.5. Other applications

In addition to their promising research as solid electrolyte and anode materials, polyphosphazenes also have cross-field exploration in other applications, including flexible solid batteries, lithium metal batteries, etc.

Lithium metal is the exemplary anode material with the highest theoretical capacity (4200 $mAh{\cdot}g^{-1}$) and the lowest electrode potential (−3.04 V vs SHE), which can meet high energy density demand [99,100]. However, the problems of internal short circuits, fire and even explosions caused by lithium dendrite hinder the popularization of lithium metal batteries [101,102]. Liebenau obtained the lithium substrate tightly covered with particle SPE by mechanically imprinting the substrate and then dropping the mixture of MEEP (Fig. 11) [103,104]. After 50 cycles, no lithium dendrite was formed, and the SPE film was not damaged. This method does not need post-treatment and is easy to operate, which is of great significance to the research of lithium metal electrodes [105].

Pearse demonstrated the fabrication and advances of the atypical atomic layer deposition (ALD) process [106] for a solid electrolyte film of lithium polyphosphazene, which was reacted between lithium tert-butoxide (LiO^tBu) and diethyl phosphoramidite (DEPA). The advancement of the ALD technology allows pinhole-free deposition even on the rough metal surface, greatly reducing the micropore between electrodes and electrolyte, and replacing the sputtering process well [107].

4. Conclusion

Polyphosphazene is a promising material for wide-ranging applications. It can be made into various structural shapes (e.g., nanospheres, nanowires), prepared by various methods (e.g., ring-opening polymerization, cationic polymerization), and designed with various functions.

With the unique chemical structure, high reactivity and multifunctional application potential, polyphosphazenes have been developed and applied in many battery components, especially as a polymer electrolyte, giving better ionic conductivity compared to PEO. But many difficulties persist, limiting practical application. The key is to find the balance between good segmental mobility (supporting high conductivity) and good mechanical stability via various processing treatments. Significant efforts are needed to achieve Li^+ ionic conductivity of 10^{-3} $S{\cdot}cm^{-1}$ at ambient temperature.

Compared with the graphite anode, the specific capacity of polyphosphazenes carbon material has been greatly improved because of in-situ heteroatom doping. However, at high temperature, heteroatoms migrate and escape, and graphitization destroys the original structure of polyphosphazenes materials, resulting in the fracture and rearrangement of atomic bonds affecting the synergistic effect of the heteroatom doping system. A possible research direction is for polyphosphazenes to be recombined with other lithium storage materials like alloy materials or transition metal oxide materials, etc., so as to change the doping mode of heteroatoms, and maintain the structure and performance of the material. The benefits of phosphonitrile in the diaphragm and other batteries is also of interest. When polyphosphazene is used as a separator in the lithium ion battery, the key problem that needs to be solved is the aggregation and shedding of polyphosphazene and its composite particles. Polyphosphazene materials have advanced significantly and are gaining increasing traction in energy storage, but mechanistic understanding of the underlying benefits (e.g., chain formation) is still amiss.

At present, research on the energy storage application of polyphosphazene materials is mostly at the laboratory level. Challenges that need to be overcome for practical industrial application include the ease of breakage of the molecular chain, low conductivity, and high cost. Concurrently, issues with respect to sustainability and environmental friendliness need to be considered.

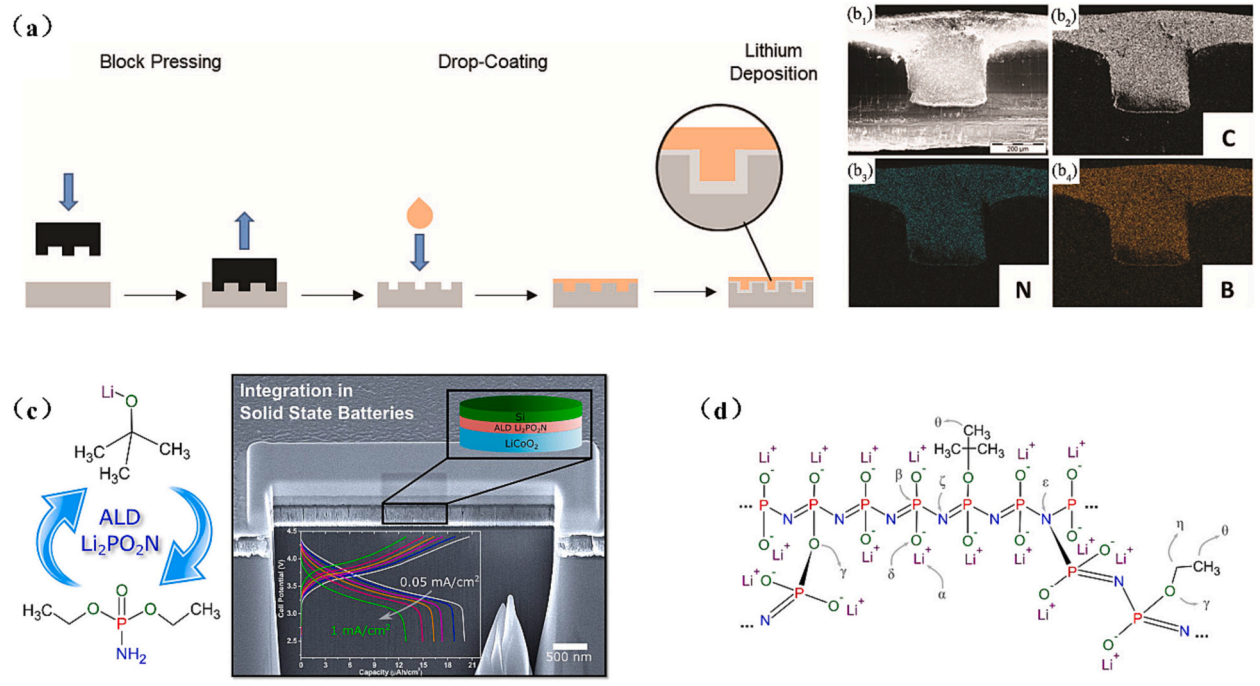

Fig. 11. (a) Scheme of the block-pressing and drop-coating processes with directed lithium deposition [103]. Copyright 2019, WILEY. (b1)–(b4) SEM images and energy spectrum analysis of the cross-section. (c) The molecular architectures of LiO^tBu and DEPA and the diagrams of membrane electrolyte [107]. (d) Schematic of the proposed molecular structure of the ALD-grown lithium polyphosphazenes [107]. Copyright 2017, American Chemical Society.

CRediT authorship contribution statement

Zhengping Zhao: Writing – review & editing, Funding acquisition, Conceptualization. **Zhao Xu:** Writing – review & editing, Writing – original draft, Investigation, Data curation. **Jiayi Chen:** Investigation. **Mingqiang Zhong:** Supervision, Project administration, Methodology. **Jiahao Wang:** Writing – review & editing, Visualization, Data curation. **Jia Wei Chew:** Project administration, Methodology, Conceptualization.

Declaration of competing interest

The authors declare that they have no known competing financial interests or personal relationships that could have appeared to influence the work reported in this paper.

Data availability

Data will be made available on request.

Acknowledgements

We are thankful for the Project Supported by Zhejiang Provincial Natural Science Foundation of China (LY21C160007) and National Natural Science Foundation of China (21504079) for the support to this research.

References

[1] H.R. Allcock, R.L. Kugel, Synthesis of high polymeric alkoxy- and aryloxyphosphonitriles, J. Am. Chem. Soc. 87 (1965) 4216–4217.
[2] X. Zhou, S. Qiu, F. Chu, Z. Xu, Y. Hu, An integrated intumescent flame retardant of bismaleimide from novel maleimide-functionalized triazine-rich polyphosphazene microspheres, Chem. Eng. J. 450 (2022) 138083.
[3] A. Romanyuk, R. Wang, A. Marin, B.M. Janus, E.I. Felner, D. Xia, Y. Goez-Gazi, K. J. Alfson, A.S. Yunus, E.A. Toth, G. Ofek, R. Carrion Jr., M.R. Prausnitz, T. R. Fuerst, A.K. Andrianov, Skin vaccination with ebola virus glycoprotein using a polyphosphazene-based microneedle patch protects mice against lethal challenge, J. Funct. Biomater. 14 (2022) 16–30.
[4] E. Quartarone, P. Mustarelli, Electrolytes for solid-state lithium rechargeable batteries: recent advances and perspectives, Chem. Soc. Rev. 40 (2011) 2525–2540.
[5] H.R. Allcock, P.E. Austin, T.X. Neenan, J.T. Sisko, P.M. Blonsky, D.F. Shriver, Polyphosphazenes with etheric side groups: prospective biomedical and solid electrolyte polymers, Macromolecules 19 (1986) 1508–1512.
[6] H.R. Allcock, P.E. Austin, Schiff base coupling of cyclic and high-polymeric phosphazenes to aldehydes and amines: chemotherapeutic models, Macromolecules 14 (1981) 1616–1622.
[7] H.R. Allcock, D.T. Welna, A.E. Maher, Single ion conductors-polyphosphazenes with sulfonimide functional groups, Solid State Ion. 177 (2006) 741–747.
[8] J. Zhou, R. Xu, C. Yin, Z. Li, W. Wu, M. Wu, In situ growth of polyphosphazene nanoparticles on graphene sheets as a highly stable nanocomposite for metal-free lithium anodes, RSC Adv. 6 (2016) 62005–62010.
[9] Z. Ali, M. Basharat, Z. Wu, A review on the morphologically controlled synthesis of polyphosphazenes for electrochemical applications, Chem. Electro. Chem. 8 (2021) 759–782.
[10] D.G. Hong, D. Jeong, C.Y. Koong, Y.-e. Han, H. Lee, J.-C. Lee, Ion-conducting cross-linked polyphosphazene binders for high-performance silicon anodes in lithium-ion batteries, ACS Applied Polymer Materials 5 (2023) 2617–2627.
[11] S. Rothemund, I. Teasdale, Preparation of polyphosphazenes: a tutorial review, Chem. Soc. Rev. 45 (2016) 5200–5215.
[12] W. Xiao, Q. Gao, M. Duan, D. Cheng, Z. Yang, An advanced hybrid fibrous separator by in-situ confining growth method for high performance lithium-ion batteries, Electrochim. Acta 433 (2022) 141209.
[13] Z. Zhou, Z. Jiang, F. Chen, T. Kuang, D. Zhou, F. Meng, Research progress in energy based on polyphosphazene materials in the past ten years, Polymers 15 (2022) 15–35.
[14] M.K. Potts, G.L. Hagnauer, M.S. Sennett, G. Davies, Monomer concentration effects on the kinetics and mechanism of the boron trichloride catalyzed solution polymerization of hexachlorocyclotriphosphazene, Macromolecules 22 (1989) 4235–4239.
[15] G.A. Carriedo, F. Alonso, P. Gomez-Elipe, J.I. Fidalgo, J. Alvarez, A. Presa-Soto, A simplified and convenient laboratory-scale preparation of 14N or 15N high molecular weight poly(dichlorophosphazene) directly from PCl_5, ChemInform 9 (2003) 3833–3836.
[16] H.R. Allcock, J.M. Nelson, R. Prange, C.A. Crane, C.D. Denus, Synthesis of telechelic polyphosphazenes via the ambient temperature living cationic polymerization of amino phosphoranimines, Macromolecules 32 (1999) 5736–5743.
[17] K. Rhili, S. Chergui, A. Samih ElDouhaibi, A. Mazzah, M. Siaj, One-pot synthesis of cyclomatrix-type polyphosphazene microspheres and their high thermal stability, ACS, Omega 8 (2023) 9137–9144.
[18] S. Mehmood, M.A. Uddin, H. Yu, L. Wang, B.U. Amin, F. Haq, S. Fahad, M. Haroon, One-pot synthesis of size-controlled poly(cyclotriphosphazene-co-hesperetin) microspheres and their properties as drug delivery carriers, ChemistrySelect 7 (2022) 273–280.
[19] H. Henke, S. Wilfert, A. Iturmendi, O. Brüggemann, I. Teasdale, Branched polyphosphazenes with controlled dimensions, J. Polym. Sci. Part A, Poly. Chem. 51 (2013) 4467–4473.
[20] B. Qamar, M. Solomon, A. Marin, T.R. Fuerst, A.K. Andrianov, S. Muro, Intracellular delivery of active proteins by polyphosphazene polymers, Pharmaceutics 13 (2021) 249–260.
[21] H.R. Allcock, J.P. Taylor, Phosphorylation of phosphazenes and its effects on thermal properties and fire retardant behavior, Polym. Eng. Sci. 40 (2000) 1177–1189.
[22] H.R. Allcock, Recent developments in polyphosphazene materials science, Curr. Opin. in Solid State Mat. Sci. 10 (2006) 231–240.
[23] S.B. Lee, S.C. Song, J.I. Jin, Y.S. Sohn, Structural and thermosensitive properties of cyclotriphosphazenes with poly(ethylene glycol) and amino acid esters as side groups, Macromolecules 34 (2001) 7565–7569.
[24] A.N. Mujumdar, S.G. Young, R.L. Merker, J.H. Magill, A study of solution polymerization of polyphosphazenes, Macromolecules 23 (1990) 14–21.
[25] N.L. Morozowich, J.L. Nichol, H.R. Allcock, Investigation of apatite mineralization on antioxidant polyphosphazenes for bone tissue engineering, Chem. Mater. 24 (2012) 3500–3509.
[26] N.L. Morozowich, T. Modzelewski, H.R. Allcock, Synthesis of phosphonated polyphosphazenes via two synthetic routes, Macromolecules 45 (2012) 7684–7691.
[27] L. Qiu, C. Zheng, Q. Zhao, Mechanisms of drug resistance reversal in dox-resistant MCF-7 cells by pH-responsive amphiphilic polyphosphazene containing diisopropylamino side groups, Mol. Pharm. 9 (2012) 1109–1117.
[28] I. Teasdale, M. Waser, S. Wilfert, F. Brüggemann, Photoreactive, water-soluble conjugates of hypericin with polyphosphazenes, Monatsh. Chem. 143 (2012) 355–360.
[29] T. Mayer-Gall, D. Knittel, J.S. Gutmann, K. Opwis, Permanent flame retardant finishing of textiles by allyl-functionalized Polyphosphazenes, ACS Appl. Mater. Interfaces 7 (2015) 9349–9363.
[30] A.L. Weikel, S.Y. Cho, N.L. Morozowich, L.S. Nair, C.T. Laurencin, H.R. Allcock, Hydrolysable polylactide-polyphosphazene block copolymers for biomedical applications: synthesis, characterization, and composites with poly(lactic-co-glycolic acid), Polym. Chem. 1 (2010) 1459–1466.
[31] H. Henke, S. Posch, O. Brueggemann, I. Teasdale, Polyphosphazene based star-branched and dendritic molecular brushes, Macromol. Rapid Commun. 37 (2016) 769–774.
[32] G.A. Carriedo, R. Campa, A.P. Soto, Front cover: polyphosphazenes-synthetically versatile block copolymers ('multi-tool') for self-assembly, Eur. J. Inorg. Chem. 2018 (2018) 2480.
[33] X. Liu, Z. Tian, C. Chen, H.R. Allcock, Synthesis and characterization of brush-shaped hybrid inorganic/organic polymers based on polyphosphazenes, Macromolecules 45 (2012) 1417–1426.
[34] J.M. Nelson, H.R. Allcock, Synthesis of triarmed-star polyphosphazenes via the 'living' cationic polymerization of phosphoranimines at ambient temperatures, Macromolecules 30 (1997) 1854–1856.
[35] L. Zhu, Y. Xu, W. Yuan, J. Xi, X. Huang, X. Tang, S. Zheng, One-pot synthesis of poly(cyclotriphosphazene-co-4,4′-sulfonyldiphenol) nanotubes via an in situ template approach, Adv. Mater. 18 (2006) 2997–3000.
[36] Z. Lu, W. Yuan, P. Yang, X. Tang, X. Huang, Preparation and characterization of novel poly[cyclotriphosphazene-co-(4,4′-sulfonyldiphenol)] nanofiber matrices, Polym. Int. 55 (2010) 1357–1360.
[37] J. Fu, X. Huang, Z. Yan, Y. Huang, Z. Lu, X. Tang, Rapid fabrication and formation mechanism of cyclotriphosphazene-containing polymer nanofibers, Eur. Polym. J. 44 (2008) 3466–3472.
[38] Z. Yan, X. Huang, W. Li, J. Fu, X. Tang, Preparation of novel hybrid inorganic–organic microspheres with active hydroxyl groups using ultrasonic irradiation via one-step precipitation polymerization, Mater. Lett. 62 (2008) 1389–1392.
[39] D.J. Chand, R.B. Magiri, H.L. Wilson, G.K. Mutwiri, Polyphosphazenes as adjuvants for animal vaccines and other medical applications, Front. Bioeng. Biotech. 9 (2021) 625482.
[40] P.M. Blonsky, D.F. Shriver, P. Austin, H.R. Allcock, Polyphosphazene solid electrolytes, J. Am. Chem. Soc. 106 (1984) 6854–6855.
[41] S. Wilfert, A. Iturmendi, H. Henke, O. Brüggemann, I. Teasdale, Thermoresponsive polyphosphazene-based molecular brushes by living cationic polymerization, Macromol. Symp. 337 (2014) 116–123.
[42] S. Qiu, W. Xing, X. Feng, B. Yu, X. Mu, R.K.K. Yuen, Y. Hu, Self-standing cuprous oxide nanoparticles on silica@polyphosphazene nanospheres: 3D nanostructure for enhancing the flame retardancy and toxic effluents elimination of epoxy resins via synergistic catalytic effect, Chem. Eng. J. 309 (2017) 802–814.
[43] M. Wang, J. Fu, D. Huang, C. Zhang, Q. Xu, Silver nanoparticles-decorated polyphosphazene nanotubes: synthesis and applications, Nanoscale 5 (2013) 7913–7919.

[44] R.C. Agrawal, G.P. Pandey, Solid polymer electrolytes: materials designing and all-solid-state battery applications: an overview, J. Phy. D-Appl. Phys. 41 (2008) 3715–3725.
[45] M. Jacob, E. Hackett, E.P. Giannelis, From nanocomposite to nanogel polymer electrolytes, J. Mater. Chem. A 13 (2002) 1–5.
[46] W.H. Meyer, Polymer electrolytes for lithium-ion batteries, Adv. Mater. 10 (1998) 439–448.
[47] M. Burjanadze, Y. Karatas, N. Kaskhedikar, L.M. Kogel, S. Kloss, A.C. Gentschev, M.M. Hiller, R.A. Mueller, R. Stolina, P. Vettikuzha, H.D. Wiemhoefer, Salt-in-polymer electrolytes for lithium ion batteries based on organo-functionalized polyphosphazenes and polysiloxanes, Z. Phys. Chemie-Int. J. Res. Phys. Chem. Chem. Phys. 224 (2010) 1439–1473.
[48] R. Meziane, J.P. Bonnet, M. Courty, K. Djellab, M. Armand, Single-ion polymer electrolytes based on a delocalized polyanion for lithium batteries, Electrochim. Acta 57 (2011) 14–19.
[49] M. Kunze, Y. Karatas, H.D. Wiemhoefer, H. Eckert, M. Schoenhoff, Activation of transport and local dynamics in polysiloxane-based salt-in-polymer electrolytes: a multinuclear NMR study, Phys. Chem. Chem. Phys. 12 (2010) 6844–6851.
[50] P.B. Balbuena, E.J. Lamas, Y.X. Wang, Molecular modeling studies of polymer electrolytes for power sources, Electrochim. Acta 50 (2005) 3788–3795.
[51] T.A. Luther, F.F. Stewart, J.L. Budzien, R.A. LaViolette, W.F. Bauer, M.K. Harrup, C.W. Allen, A. Elayan, On the mechanism of ion transport through polyphosphazene solid polymer electrolytes: NMR, IR, and Raman spectroscopic studies and computational analysis of 15N-labeled polyphosphazenes, J. Am. Chem. Soc. 107 (2003) 3168–3176.
[52] M.A. Ratner, P. Johansson, D. Shriver, Polymer electrolytes: ionic transport mechanisms and relaxation coupling, MRS Bull. 25 (2000) 31–37.
[53] D.E. Fenton, J.M. Parker, P.V. Wright, Complexes of alkali metal ions with poly (ethylene oxide), Polym. Compos. 14 (1973) 589.
[54] R.V. Morford, D.T. Welna, C. Iii, M.A. Hofmann, H.R. Allcock, A phosphate additive for poly(ethylene oxide)-based gel polymer electrolytes, Solid State Ion. 177 (2006) 721–726.
[55] Y. Tominaga, K. Yamazaki, Fast Li-ion conduction in poly(ethylene carbonate)-based electrolytes and composites filled with TiO_2 nanoparticles, Chem. Commun. 50 (2014) 4448–4450.
[56] A. Hess, G. Barber, C. Chen, T.E. Mallouk, H.R. Allcock, Organophosphates as solvents for electrolytes in electrochemical devices, ACS Appl. Mater. Interfaces 5 (2013) 13029–13034.
[57] J. Zhang, X. Huang, J. Fu, Y. Huang, W. Liu, X. Tang, Novel PEO-based composite solid polymer electrolytes incorporated with active inorganic–organic hybrid polyphosphazene microspheres, Mater. Chem. Phys. 121 (2010) 511–518.
[58] B. Wang, E. Rivard, I. Manners, A new high-yield synthesis of $cl_{(3)}P{=}NSiMe_{(3)}$, a monomeric precursor for the controlled preparation of high molecular weight polyphosphazenes, Inorg. Chem. 41 (2002) 1690–1691.
[59] J. Paulsdorf, M. Burjanadze, K. Hagelschur, H.D. Wiemhoefer, Ionic conductivity in polyphosphazene polymer electrolytes prepared by the living cationic polymerization, Solid State Ion. 169 (2004) 25–33.
[60] N. Kaskhedikar, J. Paulsdorf, M. Burjanadze, Y. Karatas, D. Wilmer, B. Roling, H. D. Wiemhofer, Ionic conductivity of polymer electrolyte membranes based on polyphosphazene with oligo(propylene oxide) side chains, Solid State Ion. 177 (2006) 703–707.
[61] Y. Karatas, W. Pyckhout-Hintzen, R. Zorn, D. Richter, H.D. Wietnhoefer, SANS investigation and conductivity of pure and salt-containing poly (bismethoxyphosphazene), Macromolecules 41 (2008) 2212–2218.
[62] J. Paulsdorf, N. Kaskhedikar, M. Burjanadze, S. Obeidi, N.A. Stolwijk, D. Wilmer, H.D. Wiemhofer, Synthesis and ionic conductivity of polymer electrolytes based on a polyphosphazene with short side groups, Chem. Mater. 18 (2006) 1281–1288.
[63] X. Zhang, J.C. Daigle, K. Zaghib, Comprehensive review of polymer architecture for all-solid-state lithium rechargeable batteries, Materials 13 (2020) 2488–2510.
[64] Y.K. Chang, H.R. Allcock, A covalently interconnected phosphazene-silicate hybrid network: synthesis, characterization, and hydrogel diffusion-related application, Adv. Mater. 15 (2003) 537–541.
[65] C.-H. Tsao, M. Ueda, P.-L. Kuo, Synthesis and characterization of polymer electrolytes based on cross linked phenoxy-containing polyphosphazenes, J. Polym. Sci. Pol. Chem. 54 (2016) 352–358.
[66] F. Croce, A.D. 'Epifanio, J. Hassoun, P. Reale, B. Scrosati, Advanced electrolyte and electrode materials for lithium polymer batteries, J. Power Sources 119 (2003) 399–402.
[67] N. Kaskhedikar, J. Paulsdorf, M. Burjanadze, Y. Karatas, B. Roling, H. D. WiemhoFer, Polyphosphazene based composite polymer electrolytes, Solid State Ion. 177 (2006) 2699–2704.
[68] M. Li, J. Lu, Z. Chen, K. Amine, 30 years of Lithium-ion batteries, Adv. Mater. 30 (2018) 1–24.
[69] Y. Zhao, X. Li, B. Yan, D. Xiong, D. Li, S. Lawes, X. Sun, Recent developments and understanding of novel mixed transition-metal oxides as anodes in lithium ion batteries, Adv. Energy Mater. 6 (2016) 1–19.
[70] J. Lu, Z. Chen, P. Feng, C. Yi, K. Amine, High-performance anode materials for rechargeable lithium-ion batteries, Electrochem. Energy Rev. 1 (2018) 35–53.
[71] C.M. Schauerman, M.J. Ganter, G. Gaustad, C.W. Babbitt, R.P. Raffaelle, B. J. Landi, Recycling single-wall carbon nanotube anodes from lithium ion batteries, J. Mater. Chem. 22 (2012) 12008–12015.
[72] Z.L. Wang, D. Xu, H.G. Wang, Z. Wu, X.B. Zhang, In situ fabrication of porous graphene electrodes for high-performance energy storage, ACS Nano 7 (2013) 2422–2430.
[73] Z. Chen, I. Belharouak, Y.K. Sun, K. Amine, Titanium-based anode materials for safe lithium-ion batteries, Adv. Funct. Mater. 23 (2013) 959–969.
[74] A. Mahmoud, J. Manuel Amarilla, K. Lasri, I. Saadoune, Influence of the synthesis method on the electrochemical properties of the $Li_4Ti_5O_{12}$ spinel in Li-half and Li-ion full-cells. A systematic comparison, Electrochim. Acta 93 (2013) 163–172.
[75] C.K. Chan, R.N. Patel, M.J. O'Connell, B.A. Korgel, Y. Cui, Solution-grown silicon nanowires for lithium-ion battery anodes, ACS Nano 4 (2010) 1443–1450.
[76] F. Luo, B. Liu, J. Zheng, G. Chu, K. Zhong, H. Li, X. Huang, L. Chen, Review-nano-silicon/carbon composite anode materials towards practical application for next generation Li-ion batteries, J. Electrochem. Soc. 162 (2015) A2509–A2528.
[77] Z. Liu, Q. Yu, Y. Zhao, R. He, M. Xu, S. Feng, S. Li, L. Zhou, L. Mai, Silicon oxides: a promising family of anode materials for lithium-ion batteries, Chem. Soc. Rev. 48 (2019) 285–309.
[78] L. Noerochim, J.-Z. Wang, S.-L. Chou, H.-J. Li, H.-K. Liu, SnO_2-coated multiwall carbon nanotube composite anode materials for rechargeable lithium-ion batteries, Electrochim. Acta 56 (2010) 314–320.
[79] B. Wang, J.S. Chen, H.B. Wu, Z. Wang, X.W.D. Lou, Quasiemulsion-templated formation of α-Fe_2O_3 hollow spheres with enhanced lithium storage properties, J. Am. Chem. Soc. 133 (2011) 17146–17148.
[80] Z.P. Zhou, F. Chen, L. Wu, T.R. Kuang, X. Liu, J. Yang, P. Fan, Z.D. Fei, Z.P. Zhao, M.Q. Zhong, Heteroatoms-doped 3D carbon nanosphere cages embedded with MoS_2 for lithium-ion battery, Electrochim. Acta 332 (2020) 135490.
[81] P. Arora, Z.J. Zhang, Battery separators, Chem. Rev. 104 (2004) 4419–4462.
[82] N. Nitta, F. Wu, J.T. Lee, G. Yushin, Li-ion battery materials: present and future, Mater. Today 18 (2015) 252–264.
[83] H. Lee, M. Yanilmaz, O. Toprakci, K. Fu, X. Zhang, A review of recent developments in membrane separators for rechargeable lithium-ion batteries, Energ. Environ. Sci. 7 (2014) 3857–3886.
[84] S.Z. Sheng, A review on the separators of liquid electrolyte Li-ion batteries, J. Power Sources 164 (2007) 351–364.
[85] S.H. Ju, Y.S. Lee, Y.K. Sun, D.W. Kim, Unique core-shell structured SiO_2 (Li^+) nanoparticles for high-performance composite polymer electrolytes, J. Mater. Chem. A1 (2013) 395–401.
[86] P. Yang, Z. Peng, C. Shi, L. Chen, J. Zhao, The functional separator coated with core-shell structured silica-poly(methyl methacrylate) sub-microspheres for lithium-ion batteries, J. Membr. Sci. 474 (2015) 148–155.
[87] Jianhui Dai, Xiu Shen, Jinbao Zhao, Chuan Shi, Daoheng Sun, A rational design of separator with substantially enhanced thermal features for lithium-ion batteries by the polydopamine-ceramic composite modification of polyolefin membranes, Energy environm. Sci. 9 (2016) 3252–3261.
[88] W. Fu, R. Xu, X. Zhang, Z. Tian, H. Huang, J. Xie, C. Lei, Enhanced wettability and electrochemical performance of separators for lithium-ion batteries by coating core-shell structured silica-poly (cyclotriphosphazene-co-4,4 '-sulfonyldiphenol) particles, J. Power Sources 436 (2019) 226839.
[89] Q. Pang, X. Liang, C.Y. Kwok, L.F. Nazar, Advances in lithium-sulfur batteries based on multifunctional cathodes and electrolytes, Nat. Energy 1 (2016) 16132.
[90] J. Park, B. Yu, J.S. Park, J.W. Choi, C. Kim, Y. Sung, J.B. Goodenough, Tungsten disulfide catalysts supported on a carbon cloth interlayer for high performance Li-S battery, Adv. Energy Mater. 7 (2017) 1602567.
[91] Z. Xiao, Z. Yang, L. Wang, H. Nie, M. Zhong, Q. Lai, X. Xu, L. Zhang, S. Huang, A lightweight TiO_2/graphene interlayer, applied as a highly effective polysulfide absorbent for fast, long-life lithium-sulfur batteries, Adv. Mater. 27 (2015) 2891–2898.
[92] R. Mukkabla, P. Meduri, M. Deepa, S.M. Shivaprasad, P. Ghosal, Sulfur enriched carbon nanotubols with a poly(3,4-ethylenedioxypyrrole) coating as cathodes for long-lasting Li-S batteries, J. Power Sources 342 (2017) 202–213.
[93] J. Luo, R.C. Lee, J.T. Jin, Y.T. Weng, C.C. Fang, N.L. Wu, A dual-functional polymer coating on a lithium anode for suppressing dendrite growth and polysulfide shuttling in Li-S batteries, Chem. Commun. 53 (2017) 963–966.
[94] W. Kong, L. Yan, Y. Luo, D. Wang, J. Wang, Li-S batteries: ultrathin MnO_2/graphene oxide/carbon nanotube interlayer as efficient polysulfide-trapping shield for high-performance Li-S batteries, Adv. Funct. Mater. 27 (2017) 1606663.
[95] Y. Lu, S. Gu, J. Guo, K. Rui, C. Chen, S. Zhang, J. Jin, J. Yang, Z.J.A.A.M. Wen, Sulfonic groups originated dual-functional interlayer for high performance lithium-sulfur battery, Acs, Appl. Mater. Interfaces 9 (2017) 14878–14888.
[96] H.W. Rollins, M.K. Harrup, E.J. Dufek, D.K. Jamison, S.V. Sazhin, K.L. Gering, D. L. Daubaras, Fluorinated phosphazene co-solvents for improved thermal and safety performance in lithium-ion battery electrolytes, J. Power Sources 263 (2014) 66–74.
[97] Y. Zheng, H. Fan, H. Li, C. Fan, H. Yuan, Z. Yang, K.C. Huang, W. Li, J. Zhang, Bifunctional separator coated with hexachlorocyclotriphosphazene/reduced graphene oxide for enhanced performance of lithium-sulfur batteries, Chemistry 24 (2018) 13582–13588.
[98] T. Lakshmikandhan, K. Sethuraman, A. Chandramohan, M. Alagar, Development of phosphazene imine-modified epoxy composites for low dielectric, antibacterial activity, and UV shielding applications, Polym. Compos. 38 (2017) E24–E33.
[99] Z. Rui, N. Li, X. Cheng, Y. Yin, Q. Zhang, Y. Guo, Advanced micro/nanostructures for lithium metal anodes, Adv. Sci. 4 (2017) 1–13.
[100] X. Shen, H. Liu, X.B. Cheng, C. Yan, J.Q. Huang, Beyond lithium ion batteries: higher energy density battery systems based on lithium metal anodes, Energy Storage Mater. 12 (2017) 161–175.
[101] P. Bieker, M. Winter, Was braucht man für eine super-batterie, Chemie in Unserer Zeit 50 (2016) 26–33.
[102] X.B. Cheng, R. Zhang, C.Z. Zhao, Q. Zhang, Toward safe lithium metal anode in rechargeable batteries: a review, Chem. Rev. 117 (2017) 10403–10473.

[103] D. Liebenau, K. Jalkanen, S. Schmohl, M.C. Stan, P. Bieker, H.-D. Wiemhoefer, M. Winter, M. Kolek, Improved interfaces of mechanically modified lithium electrodes with solid polymer electrolytes, Adv. Mater. Interfaces 6 (2019) 1900518.
[104] J.G. Park, J. Jeong, Y. Lee, M. Oh, M.H. Ryou, Y.M. Lee, Micro-patterned lithium metal anodes with suppressed dendrite formation for post lithium-ion batteries, Adv. Mater. Interfaces 3 (2016) 1600140.
[105] Y. Liu, D. Lin, P.Y. Yuen, K. Liu, J. Xie, R.H. Dauskardt, Y. Cui, An artificial solid electrolyte interphase with high Li-ion conductivity, mechanical strength, and flexibility for stable lithium metal anodes, Adv. Mater. 29 (2017) 1605531.
[106] S.M. George, Atomic layer deposition: an overview, Chem. Rev. 110 (2010) 111–131.
[107] A.J. Pearse, T.E. Schmitt, E.J. Fuller, F. El-Gabaly, C.F. Lin, K. Gerasopoulos, A. C. Kozen, A.A. Talin, G. Rubloff, K.E. Gregorczyk, Nanoscale solid state batteries enabled by thermal atomic layer deposition of a lithium polyphosphazene solid state electrolyte, Chem. Mater. 29 (2017) 3740–3753.